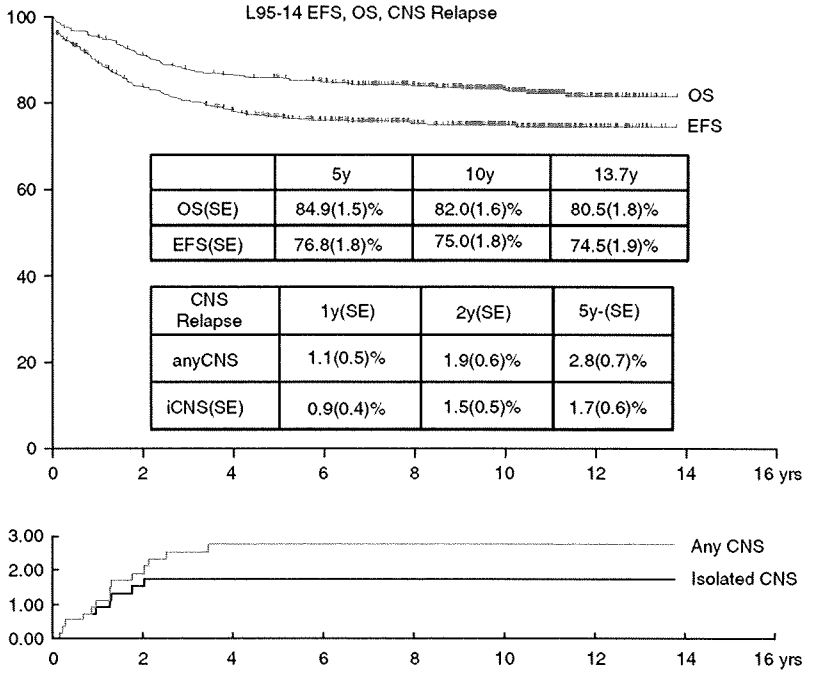

	5y	10y	13.7y
OS(SE)	84.9(1.5)%	82.0(1.6)%	80.5(1.8)%
EFS(SE)	76.8(1.8)%	75.0(1.8)%	74.5(1.9)%

CNS Relapse	1y(SE)	2y(SE)	5y-(SE)
anyCNS	1.1(0.5)%	1.9(0.6)%	2.8(0.7)%
iCNS(SE)	0.9(0.4)%	1.5(0.5)%	1.7(0.6)%

Figure 4 EFS, survival, and cumulative incidence of isolated or any CNS relapses in L95-14 study.

Conflict of interest

The authors declare no conflict of interest.

Acknowledgements

We thank Dr Tomohiro Saito and Mrs Kaori Itagaki for statistical analysis and preparing and refining the data of the protocols of ALL in TCCSG. We also thank all the pediatricians and nurses participated in the treatment and follow-up of the patients for their works. Grant of Children's Cancer Association, Japan, supported this study.

References

1 Tsuchida M, Ikuta K, Hanada R, Saito T, Isoyama K, Sugita K *et al.* Long-term follow-up of childhood acute lymphoblastic leukemia in Tokyo Children's Cancer Study Group 1981–1995. *Leukemia* 2000; **14**: 2295–2306.
2 Tsuchida M, Akatsuka J, Bessho F, Chihara H, Hayashi Y, Hoshi Y *et al.* Treatment of acute lymphoblastic leukemia in the Tokyo Children's Cancer Study Group—preliminary results of L84-11 protocol. *Acta Pediatr Jpn* 1991; **33**: 522–532.
3 Aur RJA, Simone JV, Verzosa MS, Hutsu HO, Barker LF, Pinkel DP *et al.* Childhood acute lymphocytic leukemia. *Cancer* 1978; **42**: 2133–2134.
4 Schrappe M, Beck J, Brandeis WE, Feickert HJ, Gadner H, Graf N *et al.* Treatment of acute lymphoblastic leukemia in childhood and adolescence: results of the multicenter therapy study ALL-BFM81. *Klin Padiatr* 1987; **199**: 133–150.
5 Manabe A, Tsuchida M, Hanada R, Ikuta K, Toyoda Y, Okimoto Y *et al.* Delay of the diagnostic lumbar puncture and intrathecal chemotherapy in children with acute lymphoblastic leukemia who undergo routine corticosteroid testing: Tokyo Children's Cancer Study Group study L89-12. *J Clin Oncol* 2001; **19**: 3182–3187.
6 Toyoda Y, Manabe A, Tsuchida M, Hanada R, Ikuta K, Okimoto Y, *et al.* for the Acute Lymphoblastic Leukemia Committee of the Tokyo Children's Cancer Study Group. Six months of maintenance chemotherapy after intensified treatment for acute lymphoblastic leukemia of childhood. *J Clin Oncol* 2000; **18**: 1508–1515.
7 Igarashi S, Manabe A, Ohara A, Kumagai M, Saito T, Okimoto Y *et al.* No advantage of dexamethasone over prednisolone for the outcome of standard- and intermediate-risk childhood acute lymphoblastic leukemia in the Tokyo Children's Cancer Study Group L95-14 protocol. *J Clin Oncol* 2005; **23**: 6489–6498.
8 Conter V, Aricò M, Valsecchi MG, Rizzari C, Testi AM, Messina C *et al.* Extended intrathecal methotrexate may replace cranial irradiation for prevention of CNS relapse in children with intermediate-risk acute lymphoblastic leukemia treated with Berlin-Frankfurt-Münster-based intensive chemotherapy. The Associazione Italiana di Ematologia ed Oncologia Pediatrica. *J Clin Oncol* 1995; **13**: 2497–2502.
9 Schrappe M, Reiter A, Ludwig WD, Harbott J, Zimmermann M, Hiddemann W *et al.* Improved outcome in childhood acute lymphoblastic leukemia despite reduced use of anthracyclines and cranial radiotherapy: results of trial ALL-BFM 90. German-Austrian-Swiss ALL-BFM Study Group. *Blood* 2000; **95**: 3310–3322.
10 Pui CH, Boyett JM, Relling MV, Harrison PL, Rivera GK, Behm FG *et al.* Sex differences in prognosis for children with acute lymphoblastic leukemia. *J Clin Oncol* 1999; **17**: 818–824.
11 Shuster JJ, Wacker P, Pullen J, Humbert J, Land VJ, Mahoney Jr DH *et al.* Significance of sex in childhood B-precursor acute lymphoblastic leukemia: a Pediatric Oncology Group Study. *J Clin Oncol* 1998; **16**: 2854–2863.
12 Chessells JM, Richards SM, Bailey CC, Lilleyman JS, Eden OB. Gender and treatment outcome in childhood lymphoblastic leukaemia: report from the MRC UKALL trials. *Br J Haematol* 1995; **89**: 364–372.
13 Smith M, Arthur D, Camitta B, Carroll AJ, Crist W, Gaynon P *et al.* Uniform approach to risk classification and treatment assignment for children with acute lymphoblastic leukemia. *J Clin Oncol* 1996; **14**: 18–24.
14 Ishii E, Okamura J, Tsuchida M, Kobayashi M, Akiyama Y, Nakahata T *et al.* Infant leukemia in Japan: clinical and biological analysis of 48 cases. *Med Pediatr Oncol* 1991; **19**: 28–32.
15 Isoyama K, Okawa H, Hayashi Y, Hanada R, Okimoto Y, Maeda M *et al.* Clinical and biological aspects of acute lymphoblastic leukemia in 62 infants: retrospective analysis of the Tokyo Children's Cancer Study Group. *Pediatr Int* 1999; **41**: 477–483.

16 Kosaka Y, Koh K, Kinukawa N, Wakazono Y, Isoyama K, Oda T *et al.* Infant acute lymphoblastic leukemia with MLL gene rearrangements: outcome following intensive chemotherapy and hematopoietic stem cell transplantation. *Blood* 2004; **104**: 3527–3534.
17 Riehm H, Schrappe M. Prednisone response is the strongest predictor of treatment outcome in infant acute lymphoblastic leukemia. *Blood* 1999; **94**: 1209–1217.
18 Kikuchi A, Maeda M, Hanada R, Okimoto Y, Ishimoto K, Kaneko T *et al.* Tokyo Children's Cancer Study Group (TCCSG). Moyamoya syndrome following childhood acute lymphoblastic leukemia. *Pediatr Blood Cancer* 2007; **48**: 268–272.
19 Dördelmann M, Reiter A, Zimmermann M, Fengler R, Henze G, Riehm H *et al.* Intermediate dose methotrexate is as effective as high dose methotrexate in preventing isolated testicular relapse in childhood acute lymphoblastic leukemia. *J Pediatr Hematol Oncol* 1998; **20**: 444–450.
20 Aricò M, Valsecchi MG, Rizzari C, Barisone E, Biondi A, Casale F *et al.* Long-term results of the AIEOP-ALL-95 Trial for Childhood Acute Lymphoblastic Leukemia: insight on the prognostic value of DNA index in the framework of Berlin-Frankfurt-Muenster based chemotherapy. *J Clin Oncol* 2008; **26**: 283–289.
21 Mori T, Manabe A, Tsuchida M, Hanada R, Yabe H, Ohara A *et al.* Allogeneic bone marrow transplantation in first remission rescues children with Philadelphia chromosome-positive acute lymphoblastic leukemia: Tokyo Children's Cancer Study Group (TCCSG) studies L89-12 and L92-13. *Med Pediatr Oncol* 2001; **37**: 426–431.
22 Hijiya N, Hudson M, Lensing S, Zacher M, Onciu M, Behm FG *et al.* Cumulative incidence of secondary neoplasms as the first event after treatment of childhood acute lymphoblastic leukemia increases over 30 years. *JAMA* 2007; **297**: 1207–1215.
23 Pui CH, Ribeiro RC, Hancock ML, Rivera GK, Evans WE, Raimondi SC *et al.* Acute myeloid leukemia in children treated with epipodophyllotoxins for acute lymphoblastic leukemia. *N Engl J Med* 1991; **325**: 1682–1687.
24 Pui C-H, Relling MV, Rivera GK, Hancock ML, Raimondi SC, Heslop HE *et al.* Epipodophyllotoxin-related acute myeloid leukemia—a study of 35 cases. *Leukemia* 1995; **9**: 1990–1996.
25 Silber JH, Jakachi RI, Larsen RL, Goldwein JW, Barber G. Forecasting cardiac function after anthracyclines in childhood: the role of dose, age, gender. In: Bricker JT, Green DM and D'Angio GJ (eds). *Cardiac Toxicity After Treatment for Childhood Cancer*. Wiley-Liss: New York, 1994, pp 95–102.
26 Waber DP, Urion DK, Tarbell NJ, Niemeyer C, Gelber R, Sallan SE. Late effects of central nervous system treatment of acute lymphoblastic leukemia in childhood are sex-dependent. *Dev Med Child Neurol* 1990; **32**: 238–248.
27 Schmiegelow K, Forestier E, Kristinsson J, Soderhall S, Vettenranta K, Weinshilboun R, *et al.*, on behalf of the Nordic Society of Pediatric Haematology and Oncology (NOPHO). Thiopurine methyltransferase activity is related to the risk of relapse of children of acute lymphoblastic leukemia: results from the NOPHO ALL-92 study. *Leukemia* 2009; **23**: 557–564.
28 Schmiegelow K, Al-Modhwahi I, Andersen MK, Behrendtz M, Forestier E, Hasle H, *et al.*, Nordic Society for Paediatric Haematology and Oncology. Methotrexate/6-mercaptopurine maintenance therapy influences the risk of a second malignant neoplasm after childhood acute lymphoblastic leukemia: results from the NOPHO ALL-92 study. *Blood* 2009; **113**: 6077–6084.
29 Krappmann P, Paulides M, Stöhr W, Ittner E, Plattig B, Nickel P *et al.* Almost normal cognitive function in patients during therapy for childhood acute lymphoblastic leukemia without cranial irradiation according to ALL-BFM 95 and COALL 06-97 protocols: results of an Austrian-German multicenter longitudinal study and implications for follow-up. *Pediatr Hematol Oncol* 2007; **24**: 101–109.
30 Pui CH, Campana D, Pei D, Bowman WP, Sandlund JT, Kaste SC *et al.* Treating childhood acute lymphoblastic leukemia without cranial irradiation. *N Engl J Med* 2009; **360**: 2730–2741.
31 Vilmer E, Suciu S, Ferster A, Bertrand Y, Cavé H, Thyss A *et al.* Long-term results of three randomized trials (58831, 58832, 58881) in childhood acute lymphoblastic leukemia: a CLCG-EORTC report. Children Leukemia Cooperative Group. *Leukemia* 2000; **14**: 2257–2266.
32 Gustafsson G, Schmiegelow K, Forestier E, Clausen N, Glomstein A, Jonmundsson G *et al.* Improving outcome through two decades in childhood ALL in the Nordic countries: the impact of high-dose methotrexate in the reduction of CNS irradiation. Nordic Society of Pediatric Haematology and Oncology (NOPHO). *Leukemia* 2000; **14**: 2267–2275.
33 Kamps WA, Bökkerink JP, Hählen K, Hermans J, Riehm H, Gadner H *et al.* Intensive treatment of children with acute lymphoblastic leukemia according to ALL-BFM-86 without cranial radiotherapy: results of Dutch Childhood Leukemia Study Group Protocol ALL-7 (1988–1991). *Blood* 1999; **94**: 1226–1236.
34 Gajjar A, Harrison PL, Sandlund JT, Rivera GK, Ribeirio RC, Rubnitz JE *et al.* Traumatic lumbar puncture at diagnosis adversely affects outcome in childhood acute lymphoblastic leukemia. *Blood* 2000; **96**: 3381–3384.
35 Manabe A, Ohara A, Hasegawa D, Koh K, Saito T, Kiyokawa N *et al.* Significance of the complete clearance of peripheral blasts after 7 days of prednisolone treatment in children with acute lymphoblastic leukemia: the Tokyo Children's Cancer Study Group Study L99-15. *Haematologica* 2008; **93**: 1155–1160.
36 Seibel NL, Steinherz PG, Sather HN, Nachman JB, Delaat C, Ettinger LJ *et al.* Early post-induction intensification therapy improves survival for children and adolescents with high-risk acute lymphoblastic leukemia: a report from the Children's Oncology Group. *Blood* 2008; **111**: 2548–2555.
37 Riehm H, Reiter A, Schrappe M, Berthold F, Dopfer R, Gerein V *et al.* Corticosteroid-dependent reduction of leukocyte count in blood as a prognostic factor in acute lymphoblastic leukemia in childhood (therapy study ALL-BFM 83). *Klin Padiatr* 1987; **199**: 151–160.
38 Reiter A, Schrappe M, Ludwig WD, Hiddemann W, Sauter S, Henze G *et al.* Chemotherapy in 998 unselected childhood acute lymphoblastic leukemia patients. Results and conclusions of the multicenter trial ALL-BFM 86. *Blood* 1994; **84**: 3122–3133.
39 Bostrom BC, Sensel MR, Sather HN, Gaynon PS, La MK, Johnston K *et al.*, Children's Cancer Group. Dexamethasone versus prednisone and daily oral versus weekly intravenous mercaptopurine for patients with standard-risk acute lymphoblastic leukemia: a report from the Children's Cancer Group. *Blood* 2003; **101**: 3809–3817.
40 Mitchell CD, Richards SM, Kinsey SE, Lilleyman J, Vora A, Eden TO. Medical Research Council Childhood Leukaemia Working Party. Benefit of dexamethasone compared with prednisolone for childhood acute lymphoblastic leukaemia: results of the UK Medical Research Council ALL97 randomized trial. *Br J Haematol* 2005; **129**: 734–745.

Appendix: current participating members and institutions of TCCSG (bold letter indicates authors)

M Tsuchida, Kaz Koike, K Kato, C Kobayashi: Department of Pediatric Hematology and Oncology, Ibaraki Children's Hospital, H Kigasawa: Department of Hematology and Oncology, Kanagawa Children's Medical Center, M Hashiyama: Department of Pediatrics, University of Kumamoto, School of Medicine, M Migita: Department of Pediatrics, Kumamoto Red Cross Hospital, **T Kanazawa**: Department of Pediatrics, University of Gunma, School of Medicine, A Matsui: Department of Pediatrics, Maebashi Red Cross Hospital, **H Shimada**, H Yoshihawa: Department of Pediatrics, Keio University, School of Medicine, H Kawaguchi: Department of Pediatrics, Tokyo Medical University, Ichikawa Hospital, A Makimoto, A Hosono: Department of Pediatrics, National Cancer Center Hospital, K Takagi, S Morinaga: Department of Pediatrics, National Hospital Organization Kumamoto Medical Center, **M Kumagai**,

C Kiyotani, **T Mori**, Y Shiota: Department of Pediatric Hematology/Oncology, National Center for Child Health and Development, International Medical Center, K Moriwaki: Department of Pediatrics, Saitama Medical University, Medical Center, **K Ko**, **Y Hanada**, S Mochizuki, D Toyama: Department of Hematology/Oncology, Saitama Children's Medical Center, **M Akiyama**, Y Kato, Y Hoshi: Department of Pediatrics, Tokyo Jikei University, School of Medicine,Y Gunji, Y Kashii, T Morimoto: Department of Pediatrics, Jichi Medical School, M Saito, J Fujimura, K Ishimoto: Department of Pediatrics, Juntendo University, School of Medicine, Tokyo, K Isoyama, M Yamamoto, T Hirota: Department of Pediatrics, Showa University, School of Medicine, Fujigaoka Hospital, Ken Koike, R Yanagisawa, **M Shiobara**: Department of Pediatrics, University of Shinshu, School of Medicine, E Ishii: Department of Hematology/Oncology, Nagano Children's Hospital, A Kinoshita, K Kondo, M Morimoto: Department of Pediatrics, St Marianna University School of Medicine, **Y Hosoya**, **C Ogawa**, Y Ishida, **A Manabe**, M Ozawa, D Hasegawa, T Kamiya: Department of Pediatrics, St Luke's International Hospital, Tokyo, H Ochiai, Y Sato, E Sakao, K Ito: Department of Pediatrics, Chiba University, School of Medicine, Chiba, K Sunami, **Y Noguchi**, T Igarashi: Department of Pediatric Hematology/Oncology, Narita Red Cross Hospital, I Komori: Department of Pediatrics, Matsudo City Hospital, **S Oota**: Department of Pediatrics, Teikyo University, Chiba Medical Center, **Y Okimoto**, H Kakuta: Department of Hematology/Oncology, Chiba Children's Hospital, S Kato, K Morimoto, **S Yabe**, M Yabe: Department of Pediatrics and Blood Transfusion, Tokai University, School of Medicine, S Mizutani, **M Kajiwara**, M Nagasawa, **D Tomizawa**: Department of Pediatrics, Tokyo Medical and Dental University, School of Medicine, Tokyo, S Koana, Y Kashiwagi: Department of Pediatrics, Tokyo Medical University Hospital, **K Ida**, J Takita, K M Kato, K Ooki: Department of Pediatrics, Tokyo University, School of Medicine, E Wada, F Kato: Department of Pediatrics, Tokyo Women's Medical College, East Medical Center, **A Ohara**, Y Kojima, K Mitsui, Y Uchino: Department of First Pediatrics, Toho University Medical Center, Oomori Hospital, A Watanabe: Department of Second Pediatrics, Toho University Medical Center, Oomori Hospital, **K Sugita**, K Fukushima, H Kurosawa, S Hagisawa, Y Sato: Department of Pediatrics, Dokkyo Medical College, Tochigi, **T Kaneko**, K Fukuoka, M Sugita: Department of Hematology/Oncology, Tokyo Metropolitan Kiyose Children's Hospital, H Kaku, M Kawamura: Department of Pediatrics, Tokyo Metropolitan Komagome Hospital, **M Maeda**, Y Fukunaga, S Migita, T Ueda: Department of Pediatrics, Nippon Medical School, K Asano: Department of Pediatrics, Nippon Medical School Chiba Hokusoh Hospital, K Sugita, **T Inukai**, K Goi: Department of Pediatrics: University of Yamanashi Hospital, **H Goto**, H Fugii, K Ikuta, M Yanagimachi, T Yokosuka: Department of Pediatrics, Yokohama City University, School of Medicine, S Kai, **H Takahashi**, A Goto, F Tanaka: Department of Pediatrics, Yokohama Saiseikai Nanbu Hospital, Yokohama, K Tsuji, Y Ebihara: Department of Pediatric, Blood Transfusion, The University of Tokyo, The Institute of Medical Science, N Nakadate: Department of Pediatrics, Kitazato University, School of Medicine, Y Ishiguro, T Suzuki: Department of Pediatrics, Teikyo University, Mizonokuchi Hospital, **K Fukushima**, S Nakao: Department of Pediatrics, Tsukuba University Hospital, **Y Hayashi**, M Sotomatsu, A Paku: Department of Hematology/Oncology, Gunma Chidren's Hospital, F Bessho, H Yoshino, M Ishii, Y Genma: Department of Pediatrics, Kyorin University, School of Medicine, Tokyo, K Kogawa, Y Tsuji, K Imai: Department of Pediatircs, National Defense Medical college, F Sawa: Department of Pediatrics, Saiseikai Yokohama City, Tobu Hospital, Yokohaya.

Leukemia (2009) 23, 2197–2209

www.nature.com/leu

LEADING ARTICLE

Mixed-lineage-leukemia (*MLL*) fusion protein collaborates with Ras to induce acute leukemia through aberrant *Hox* expression and Raf activation

R Ono[1,2,3], H Kumagai[1], H Nakajima[4,5], A Hishiya[1,2], T Taki[6], K Horikawa[7], K Takatsu[7,8], T Satoh[9], Y Hayashi[10], T Kitamura[2] and T Nosaka[1,2,3]

[1]*Division of Hematopoietic Factors, The Institute of Medical Science, The University of Tokyo, Tokyo, Japan;* [2]*Division of Cellular Therapy, The Institute of Medical Science, The University of Tokyo, Tokyo, Japan;* [3]*Department of Microbiology and Molecular Genetics, Mie University Graduate School of Medicine, Mie, Japan;* [4]*Center of Excellence, The Institute of Medical Science, The University of Tokyo, Tokyo, Japan;* [5]*Division of Hematology, Department of Internal Medicine, Keio University School of Medicine, Tokyo, Japan;* [6]*Department of Molecular Laboratory Medicine, Kyoto Prefectural University of Medicine Graduate School of Medical Science, Kamigyo-ku, Kyoto, Japan;* [7]*Department of Immunology, The Institute of Medical Science, The University of Tokyo, Tokyo, Japan;* [8]*Department of Immunobiology and Pharmaceutical Genetics, Graduate School of Medicine and Pharmaceutical Sciences, University of Toyama, Toyama, Japan;* [9]*Division of Molecular Biology, Department of Biochemistry and Molecular Biology, Kobe University Graduate School of Medicine, Kobe, Japan and* [10]*Gunma Children's Medical Center, Gunma, Japan*

Mixed-lineage-leukemia* (*MLL*) fusion oncogenes are closely involved in infant acute leukemia, which is frequently accompanied by mutations or overexpression of *FMS-like receptor tyrosine kinase 3* (*FLT3*). Earlier studies have shown that *MLL* fusion proteins induced acute leukemia together with another mutation, such as an *FLT3* mutant, in mouse models. However, little has hitherto been elucidated regarding the molecular mechanism of the cooperativity in leukemogenesis. Using murine model systems of the *MLL*-fusion-mediated leukemogenesis leading to oncogenic transformation *in vitro* and acute leukemia *in vivo*, this study characterized the molecular network in the cooperative leukemogenesis. This research revealed that *MLL* fusion proteins cooperated with activation of Ras *in vivo*, which was substitutable for Raf *in vitro*, synergistically, but not with activation of signal transducer and activator of transcription 5 (STAT5), to induce acute leukemia *in vivo* as well as oncogenic transformation *in vitro*. Furthermore, *Hoxa9*, one of the *MLL*-targeted critical molecules, and activation of Ras *in vivo*, which was replaceable with Raf *in vitro*, were identified as fundamental components sufficient for mimicking *MLL*-fusion-mediated leukemogenesis. These findings suggest that the molecular crosstalk between aberrant expression of *Hox* molecule(s) and activated Raf may have a key role in the *MLL*-fusion-mediated-leukemogenesis, and may thus help develop the novel molecularly targeted therapy against *MLL*-related leukemia.

Leukemia (2009) **23**, 2197–2209; doi:10.1038/leu.2009.177; published online 27 August 2009
Keywords: MLL; Ras; MAP kinase; leukemogenesis

Introduction

Multistep oncogenesis has been suggested in malignancy by the observation of more than two heterogeneous genetic and/or epigenetic lesions.[1] In leukemogenesis, recurring chromosomal translocations are frequently found in hematological malignancies, which sometimes coincide with subtle but critical genetic mutations leading to functional aberration.[2–4] Earlier studies showed that many of the translocation target genes are transcription factors involved in hematopoietic differentiation and/or self-renewal, whereas coincident mutations often occur on the genes involved in cell proliferation.[4] These results lead to a hypothetical model of leukemogenesis in which these two kinds of genetic alterations may cooperate to induce acute leukemia. This concept has been recently exemplified in experimental models using combinations of fusion genes, including *mixed-lineage leukemia* (*MLL*, also called *ALL1* or *HRX*) or *AML1* fusion genes, and other coincident genetic mutations.[5–9]

MLL is a proto-oncogene that is rearranged in human acute leukemia with chromosome 11 band q23 (11q23) translocation,[10,11] encoding a histone methyltransferase that assembles in a chromatin-modifying supercomplex.[12] Meanwhile, *MLL* fusion gene leads to leukemogenesis through several *HOX* genes directly transactivated by *MLL* fusion protein itself.[4,11,13,14] It is noteworthy that most of the genetically engineered mice carrying the *MLL* fusion developed hematological malignancy after a long latency, suggesting that secondary genotoxic stress is required to develop overt acute leukemia.[15–18] An earlier study presented direct evidence that *MLL* fusion proteins induced myeloproliferative disease (MPD) with a long latency, and caused acute leukemia with a short latency together with a coincident mutation of *FMS-like tyrosine kinase 3* (*FLT3*).[6]

Recent studies revealed that genetic alterations, including *FLT3*, *NRAS* (neuroblastoma RAS viral (v-ras) oncogene homolog) and *KRAS* (v-Ki-ras2 Kirsten rat sarcoma viral oncogene homolog), are frequently accompanied by 11q23 translocation.[19,20] *FLT3* is a receptor tyrosine kinase involved in leukemogenesis and normal hematopoiesis.[21] The mutations of *FLT3* are mainly classified into length mutations such as internal tandem duplication (ITD) of the juxtamembrane domain, and point mutations within the activation loop of the second tyrosine kinase domain (TKD).[21] Interestingly, *FLT3*-TKD, as well as overexpression of the wild type of FLT3, is found to be frequently associated with infant acute lymphoid leukemia (ALL), with rearrangements of *MLL*.[19,22] Both types of *FLT3* mutations result in a constitutive activation of *FLT3* kinase activity, followed by activation of signaling pathways, including signal transducer and activator of transcription 5 (STAT5) and Ras/Raf/mitogen-activated protein (MAP) kinase.[23,24] Both STAT5 and Ras/Raf/MAP kinase (MAPK) are involved in cellular

Correspondence: Dr T Nosaka, Department of Microbiology and Molecular Genetics, Mie University Graduate School of Medicine, 2-174 Edobashi, Tsu, Mie 514-8507, Japan.
E-mail: nosaka@doc.medic.mie-u.ac.jp
Received 1 October 2008; revised 17 July 2009; accepted 21 July 2009; published online 27 August 2009

proliferation, survival and differentiation.[25,26] Constitutively active mutants of Ras induce oncogenic transformation through activation of the MAPK cascade.[26] However, little has so far been elucidated regarding the molecular mechanism of collaboration in leukemogenesis.

To further clarify the molecular mechanism of *MLL*-fusion-mediated leukemogenesis, we focused on signal transduction associated with malignant transformation that collaborates with *MLL* fusion protein *in vitro*, and highlighted the contrastive roles of STAT5 and MAPK in leukemogenesis. Interestingly, comparative analyses suggested synergistic collaboration with activated Ras in *MLL*-fusion-mediated leukemogenesis, and also activation of Raf in malignant transformation *in vitro*, but not with STAT5 activation *in vivo* and *in vitro*. Thus, the activation of Ras/Raf/MAPK cascade may have an important role in multistep leukemogenesis with 11q23 translocations.

Materials and methods

Construction of the plasmids and retrovirus production

Fragments of murine constitutively active mutants of STAT5A (#2[27] and 1*6[28]) fused with a FLAG tag at the C-terminus, a coding region of human $NRAS^{G12V}$ and *MLL-eleven nineteen leukemia* (*ENL*) short form[6] were inserted upstream of the internal ribosomal entry site (IRES)-enhanced green fluorescent protein (EGFP) cassette of pMYs-IRES-EGFP.[29] Fragments of coding regions of a wild type of *NRAS* and $NRAS^{G12V}$ were inserted into pMXs-puro.[29] A fragment of murine *Hoxa9*[30] (a kind gift from Dr G Sauvageau) was inserted into pMXs-IRES-EGFP.[29] A fragment of a dominant negative mutant (dn) of STAT5A[23] was inserted upstream of the IRES-Kusabira-Orange (KO)[31] cassette of pMXs-IRES-KO, in which the EGFP cassette in pMXs-IRES-EGFP[29] was replaced with the KO cassette of phKO1-S1 (MBL, Nagoya, Japan). pMXs-neo-*MLL-SEPT6*,[6] pMY-FLT3-ITD-IRES-EGFP,[6] pMY-$FLT3^{D835V}$-IRES-EGFP[6] and pBabe-puro-Δ*Raf*-estrogen receptor (ER)[28] were described earlier. Retroviruses were harvested 48 h after transfection with each retroviral construct into PlatE cells[29] in which appropriate expression of the transgenes was confirmed by western blot analysis, as described earlier.[6]

Cells

An *MLL-SEPT6*-immortalized murine myelomonocytic cell line, HF6, was established through colony-replating assays using retroviral transduction with pMXs-neo-*MLL-SEPT6* as described earlier.[6] A *Hoxa9*-immortalized murine myelomonocytic cell line, A9G, was established through infection with retroviruses harboring *Hoxa9* in pMXs/IRES-EGFP[29] as reported earlier.[32] The HF6,[6] A9G and murine pro-B Ba/F3[28] cells were cultured in the presence of interleukin-3 (IL-3) (R&D Systems, Minneapolis, MN, USA). HF6 cells transduced with *FLT3* mutants were cultured in the same medium, except for the absence of IL-3. The expression levels of *FLT3* in these cells were evaluated using a phycoerythrin (PE)-conjugated anti-CD135 antibody, or an anti-mouse immunoglobulin G1,κ, as the isotype-matched control (BD Biosciences, San Diego, CA, USA) using fluorescence-activated cell sorting (FACS) Calibur (BD Biosciences) as described earlier.[33]

Immunoprecipitation and western blot analysis

Fifty million parental and additionally transduced HF6 cells, or 10 million parental and transduced Ba/F3 cells, were harvested in the lysis buffer, and the lysates were either suspended with 1 × sodium dodecyl sulfate sample buffer after immunoprecipitation using polyclonal anti-STAT5A antibody (L-20) (Santa Cruz Biotechnology, Santa Cruz, CA, USA) or directly mixed with an equal volume of 2 × sodium dodecyl sulfate sample buffer and then boiled, as described earlier.[25] In some experiments, the parental HF6 cells had been deprived of IL-3 8 h before harvest. Western blot analysis of each sample was performed using the polyclonal anti-STAT5A (L-20), monoclonal anti-phosphotyrosine (4G10) (Upstate Biotechnology, Lake Placid, NY, USA), polyclonal anti-extracellular signal-related kinase (ERK)1/2, monoclonal anti-phospho-ERK1/2 (E10) (Cell Signaling Technology, Danvers, MA, USA), monoclonal anti-α-tubulin (Sigma-Aldrich, St Louis, MO, USA), monoclonal anti-FLAG (M2), polyclonal anti-ERα (MC-20) and monoclonal anti-N-Ras (F155) (Santa Cruz Biotechnology) antibodies to probe membranes, as described earlier.[25]

Evaluation of cellular effects by inhibition of signal transduction in vitro

The response to the drug was evaluated as described earlier.[23] In brief, HF6 cells expressing the *FLT3* mutants (3×10^5) were infected with retroviruses harboring or not harboring the dnSTAT5A in pMXs-IRES-KO in the presence of polybrene, as described earlier.[6] Viable cell numbers were counted with standard Trypan blue staining, and the expression of the dnSTAT5A was monitored by assessment of KO positivity using the FL2 channel on the FACS Calibur, daily after infection. At 48 h after infection, to evaluate the status of phosphorylated STAT5, half a million of these cells were fixed with fixation buffer, permeablized with Perm Buffer III and analyzed with an Alexa Fluor 647-conjugated anti-phospho-STAT5 (Y694) (all from BD Biosciences) antibody, or the anti-mouse immunoglobulin G1,κ, as the isotype-matched control antibody, using the FL4 channel on the FACS Calibur, according to the manufacturer's recommendation. As controls, the parental HF6 cells with and without IL-3 stimulation after deprivation of IL-3 for 8 h were used. Meanwhile, these HF6 cells (1×10^4) were cultured for 72 h in 24-well plates in the presence of various concentrations of a MAPK kinase (MEK) inhibitor, U0126, or a PI3 kinase inhibitor, LY294002 (Calbiochem-Novabiochem, San Diego, CA, USA) and each vehicle control (ethanol for U0126 and dimethyl sulfoxide for LY294002). Viable cell numbers were counted with standard Trypan blue staining after each treatment, followed by calculation of the 50% inhibitory concentration (IC50) of each drug using a logistic regression model. To evaluate the inhibitory effect of U0126 on ERK1/2, five million of the cells were treated for 2 h, harvested and analyzed with the anti-ERK1/2 or the anti phospho-ERK1/2 antibody after western blotting.

Myeloid transformation assays in vitro

In a series of transformation assays, the acquisition of IL-3-independent proliferation was examined in IL-3-dependent cells. HF6 and Ba/F3 cells were infected with retroviruses harboring *NRAS*, $NRAS^{G12V}$ or mock in pMXs-puro; Δ*Raf*-ER or mock in pBabe puro; and STAT5A1*6, STAT5A#2 or none (only GFP) in pMYs-IRES-EGFP, respectively, in the presence of polybrene, as described earlier.[6] A9G cells were also retrovirally transduced with *NRAS*, $NRAS^{G12V}$ Δ*Raf*-ER or each mock in the same way. For puromycin selection, the transduced cells were cultured with 1 μg/ml of puromycin 24–96 h after infection, followed by propagation for 5 days in the absence of puromycin.

Next, 1×10^5 puromycin-resistant cells transduced with *NRAS*, *NRAS*^{G12V} or mock were cultured in 24-well plates in the absence of IL-3, whereas those transduced with Δ*Raf*-ER or mock were cultured under the same condition, except for the presence of 1 μM of 4-hydroxy-tamoxifen or a vehicle control (ethanol). The cells transduced with STAT5A1*6, STAT5#2 or none were purified on the basis of the expression of GFP using a FACS Aria (BD Biosciences) 36 h after infection. Immediately, these purified cells (1×10^4) were cultured in 96-well plates in the absence of IL-3, to avoid excessive signals caused by STAT5A#2 or 1*6 in the presence of IL-3, which led to cell death as described earlier.[25] Viable cell numbers were counted periodically after standard Trypan blue staining.

Leukemogenesis assays in vivo

Leukemogenesis assays *in vivo* using C57BL/6 mice produced by a combination of two kinds of transgenes were performed with lethal conditioning using lethally (9.5 Gy) irradiated recipients, or with sublethal conditioning using sublethally (5.25 Gy) irradiated recipients receiving no radioprotective bone marrow (BM) cells, as described earlier[6] (Supplementary Figure 1). In brief, hematopoietic progenitors were harvested from 6- to 10-week-old Ly-5.1 C57BL/6 mice 4 days after intraperitoneal administration of 150 mg/kg 5-fluorouracil, and cultured overnight in alpha minimal essential medium supplemented with 20% fetal calf serum and 50 ng/ml each of mouse stem cell factor, human IL-6, human FLT3-ligand (R&D Systems) and human thrombopoietin (Kirin Brewery, Takasaki, Japan). The prestimulated cells were infected with several combinations of the retroviruses for 60 h in the α minimal essential medium supplemented with the same fetal calf serum and cytokines using RetroNectin (Takara Bio Inc., Otsu, Japan) according to the manufacturer's recommendations, followed by intravenous injection of 10^5 of the cells into Ly-5.2 mice together with either a radioprotective dose (2×10^5) of Ly-5.2 cells under lethal conditioning or none under sublethal conditioning. Morbid mice and their tissue samples were analyzed, and immunophenotyping of BM, splenic and thymic cells was performed using the FACS Calibur, as described earlier.[33] The hematopoietic neoplasms were diagnosed mainly on the basis of morphology as described earlier.[6] The probabilities of murine overall survival were estimated using Kaplan–Meier method and compared using the log-rank test. All animal studies were performed in accordance with the guidelines of the Animal Care Committees of the Institute of Medical Science, the University of Tokyo and the Mie University.

Southern blot analysis

Genomic DNA was extracted from spleens, digested with *Nhe*I or *Bam*HI for detecting proviral integration and clonality, respectively, and analyzed with the Neo or puro probe (Supplementary Figure 1) as described earlier.[34]

Reverse transcriptase-polymerase chain reaction (PCR)

Total RNA was extracted from cell lines, spleen or BM, and reverse transcribed to complementary DNA as described earlier.[6] The conditions, reagents for reverse transcriptase-PCR and the primers specific for *β*$_2$*microglobulin* (*β*$_2$*MG*), *Hoxa9* and *MLL-SEPT6* have been described earlier,[6] except that PCR amplification for *MLL-SEPT6* transcripts was sometimes run for 35 cycles. To detect the transcript of *NRAS*^{G12V}, PCR amplification was run for 21 cycles using the following primers: *NRAS-S*, 5′-GTGGTTATAGATGGTGAAACCTGTT-3′ and *NRAS-AS*, 5′-GACCATAGGTACATCTTCAGAGTCCT-3′.

Results

MLL-SEPT6 *cooperates with both types of* FLT3 *mutations through different modes of signal transduction*

To clarify the molecular mechanism of cooperation between *MLL* fusion proteins and *FLT3* mutants, signaling pathways of *FLT3*-ITD and *FLT3*-TKD that cooperate with *MLL-SEPT6* were examined using the IL-3-dependent *MLL-SEPT6*-immortalized cell line, HF6.[6] Earlier, STAT5 and MAPK ERK1/2 had been found to be activated downstream of *FLT3* mutants in factor-dependent cell lines.[23,24] Therefore, the activation of these molecules was first examined using parental HF6 and transformed HF6 cells expressing FLT3-*ITD* (HF6^{ITD}) or *FLT3*^{D835V} (HF6^{D835V}) described earlier.[6] Nearly equal levels of expression of the *FLT3* mutants in the transformed HF6 cells were confirmed (Figure 1a). A western blot analysis after immunoprecipitation of the lysates from these cells revealed constitutive phosphorylation of STAT5A in HF6 cells expressing the FLT3 mutants in the absence of IL-3, but little in the parental HF6 cells that had been deprived of IL-3 (Figure 1b). In addition, a western blot analysis of the same lysates also revealed constitutive phosphorylation of ERK1/2 in those cells expressing the *FLT3* mutants, but little in the parental HF6 cells that had been deprived of IL-3 (Figure 1b).

Next, to determine whether STAT5 and/or MAPK were important in the transformation of HF6 cells expressing *FLT3* mutants, each signaling pathway was inhibited using dnSTAT5A or MEK inhibitor U0126. After retroviral transduction with the dnSTAT5A, the proliferation of HF6^{ITD} cells expressing dnSTAT5A was suppressed more efficiently than that of HF6^{D835V} cells expressing dnSTAT5A (Figure 2a). KO-positive cells expressing dnSTAT5A showed higher levels of phosphorylated STAT5 than KO-negative cells (Figure 2b). This finding is consistent with the earlier report showing that the dnSTAT5A exerts its effect on endogenous STAT5A and 5B with persistent phosphorylation of the dnSTAT5A itself.[35] In contrast, U0126 retarded the proliferation of the HF6^{D835V} cells more effectively than the HF6^{ITD} cells (Figure 2c, each IC50 is 0.67 ± 0.35 μM for HF6^{D835V} and 6.09 ± 0.90 μM for HF6^{ITD} in the absence of IL-3). Indeed, U0126 inhibited phosphorylation of ERK1/2 in the HF6^{ITD} and HF6^{D835V} cells in a semidose-dependent manner (Figure 2d). In addition, another important signaling pathway downstream of *FLT3*, through PI3 kinase, was inhibited using LY294002. LY294002 also retarded the growth of the HF6^{D835V} and HF6^{ITD} cells in a dose-dependent manner, but there was no remarkable difference between both types of HF6 cells (Supplementary Figure 2, each IC50 is 4.18 ± 0.55 μM for HF6^{D835V} and 8.12 ± 1.54 μM for HF6^{ITD} in the absence of IL-3).

Taken together, these results *in vitro* suggested that the activation of MAPK was more critical for transformation by *FLT3*-TKD than by *FLT3*-ITD in HF6 cells, whereas activation of STAT5 was more critical for transformation by *FLT3*-ITD than by *FLT3*-TKD.

Activation of Ras-MAPK cascade enables HF6 cells to grow without IL-3 through cooperation between Hoxa9 *and Raf*

We further examined whether direct activation of either STAT5 or MAPK cascade is sufficient to confer factor-independent

growth on HF6 cells. Although the constitutively active mutants of STAT5A, the relatively stronger mutant STAT5A1*6 and weaker mutant STAT5A#2, enabled Ba/F3 cells (Ba/F3^{1*6}, Ba/F3$^{\#}$) to grow without IL-3 as reported earlier,[25,27,28] both failed to confer factor-independent growth on HF6 cells with limited elongation of survival time without IL-3 (Figures 3a and c). In contrast, the oncogenic *NRAS* mutant, *NRAS*^{G12V}, which had been detected in a case of *AML* with *MLL-SEPT6*,[20] enabled HF6 cells (HF6^{G12V}) to grow without IL-3, while it conferred no factor-independent growth on Ba/F3 with limited elongation of survival time without IL-3 (Figures 3b and c). In addition, Raf-1, a signal molecule downstream of Ras in Ras-MAPK cascades associated with malignant transformation, was tested with an activation-inducible system using Δ*Raf*-ER, consisting of the catalytic domain of human RAF-1 (ΔRaf) and the hormone-binding domain of the ER (Figure 3d), as described earlier.[28] Unlike transduced Ba/F3 (Ba/F3$^{\Delta Raf\text{-}ER}$) cells, transduced HF6 (HF6$^{\Delta Raf\text{-}ER}$) cells grew without IL-3 only in the presence of 4-hydroxy-tamoxifen (Figure 3e). In these HF6$^{\Delta Raf-ER}$ cells treated with 4-hydroxy-tamoxifen, STAT5A was not found to be secondarily activated by induction of activation of Raf/MAPK cascade in the absence of IL-3, whereas it was found to be weakly activated by stimulation with IL-3 for 15 min (data not shown).

Furthermore, we examined whether *Hoxa9*, which is one of the well-known target genes of *MLL* fusion proteins,[10,11,13,14] is involved in cooperation between *MLL* fusion protein and Ras/Raf/MAPK cascade. In the myeloid transformation assays, the murine BM progenitors immortalized by *Hoxa9* in the presence of IL-3 (named A9G) proliferated without IL-3 after retroviral transduction of *NRAS*^{G12V} (Figure 3b). In the inducible transformation system using Δ*Raf*-ER, transduced A9G

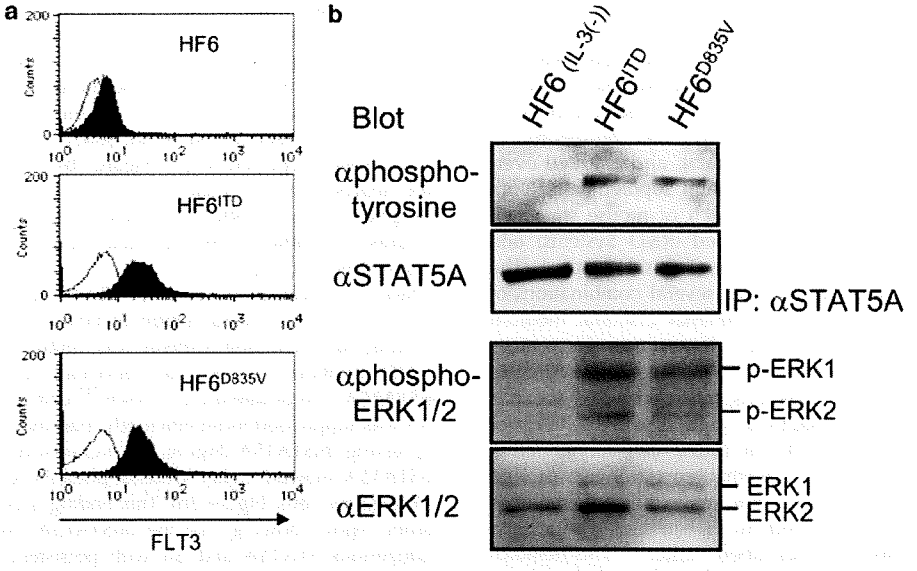

Figure 1 Characterization of signal transduction in the HF6 cells transformed by *FMS-like receptor tyrosine kinase 3* (*FLT3*) mutants. (**a**) Expression of each *FLT3* mutant in HF6 and their transformed cells. The shadow profiles and black lines represent fluorescence-activated cell sorting (FACS) staining obtained using the antibody specific to *FLT3* and its isotype control antibody, respectively. (**b**) Western blot analyses of proteins extracted from HF6 and their transformed cells after immunoprecipitation using the anti-signal transducer and activator of transcription 5A (STAT5A) antibody (upper two panels), and of the whole lysates (lower two panels). The parental HF6 cells had been deprived of interleukin-3 (IL-3) 8 h before harvest. The blot of the immunoprecipitated samples was probed with the anti-STAT5A antibody (upper bottom panel), followed by reprobe with 4G10 (the anti-phosphotyrosine antibody) (upper top panel). The blot of the whole lysates was probed with the anti-extracellular signal-related kinase (ERK)1/2 antibody (lower bottom panel), followed by reprobe with the anti-phospho-ERK1/2 antibody (lower top panel).

Figure 2 Differential effects of inhibition of cellular signal transduction on the HF6 cells transformed by *FMS-like receptor tyrosine kinase 3* (*FLT3*) mutants. (**a**) Effect of the retroviral transduction with the dominant negative mutant of signal transducer and activator of transcription 5A (dnSTAT5A) in pMXs-internal ribosomal entry site (IRES)-Kusabira-Orange (KO) on the transformed and parental HF6 cells. Viable cell numbers and KO expression were monitored daily after the transduction, and the averages of ratios of each KO-positive cell number at days 1, 2, 3 and 4 to that at day 1 are shown with s.d. (bars). (**b**) Intracellular flow cytometric analyses of phospho-STAT5 (Y694) on the transformed and parental HF6 cells transduced with dnSTAT5A in pMXs-IRES-KO. The density plots show expression of each intracellular antigen labeled with the Alexa Fluor 647-conjugated anti-phospho-STAT5 (Y694) (upper eight panels) or its isotype control (lower two panels) antibody versus expression of KO. As negative controls, nontransduced and mock-transduced HF6 cells were used, respectively (lower two panels using the isotype control antibody). As references, nontransduced HF6 cells were deprived of interleukin-3 (IL-3) for 8 h (HF6 (IL-3(−))), or stimulated with IL-3 for 15 min after the same deprivation (HF6 (IL-3(+))), and then used (lower two panels using the anti-phospho-STAT5 antibody). KO and Alexa Fluor 647 were detected using the FL2 and FL4 channels of the fluorescence-activated cell sorting (FACS) Calibur, respectively. (**c**) Effect of the various concentrations of mitogen-activated protein kinase (MAPK) kinase (MEK) inhibitor, U0126, on the transformed and the parental HF6 cells. The averages with s.d. (bars) of ratios of viable cell numbers in the presence of each concentration of U0126 to those in the absence of U0126 are shown. (**d**) Western blot analyses of the whole lysates extracted from the transformed HF6 cells treated with U0126. Both groups of transformed HF6 cells were treated with various concentrations (shown above each upper panel) of U0126 for 2 h and then harvested. Both blots were probed with the anti-phospho-extracellular signal-related kinase (ERK)1/2 antibody (each top panel), followed by reprobe with the anti-ERK1/2 antibody (each bottom panel).

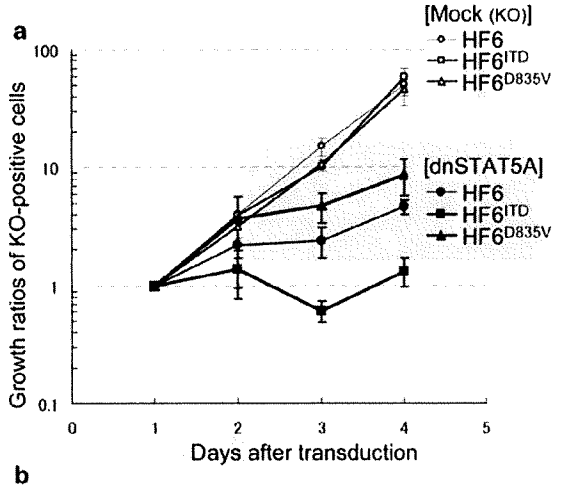
a
[Mock (KO)]
HF6
HF6ITD
HF6D835V
[dnSTAT5A]
HF6
HF6ITD
HF6D835V
Growth ratios of KO-positive cells
Days after transduction

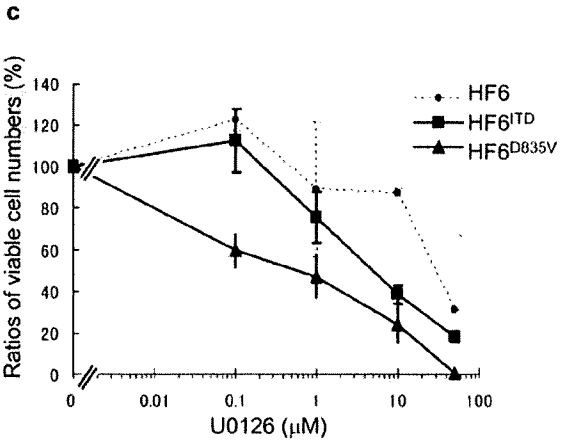
c
HF6
HF6ITD
HF6D835V
Ratios of viable cell numbers (%)
U0126 (μM)

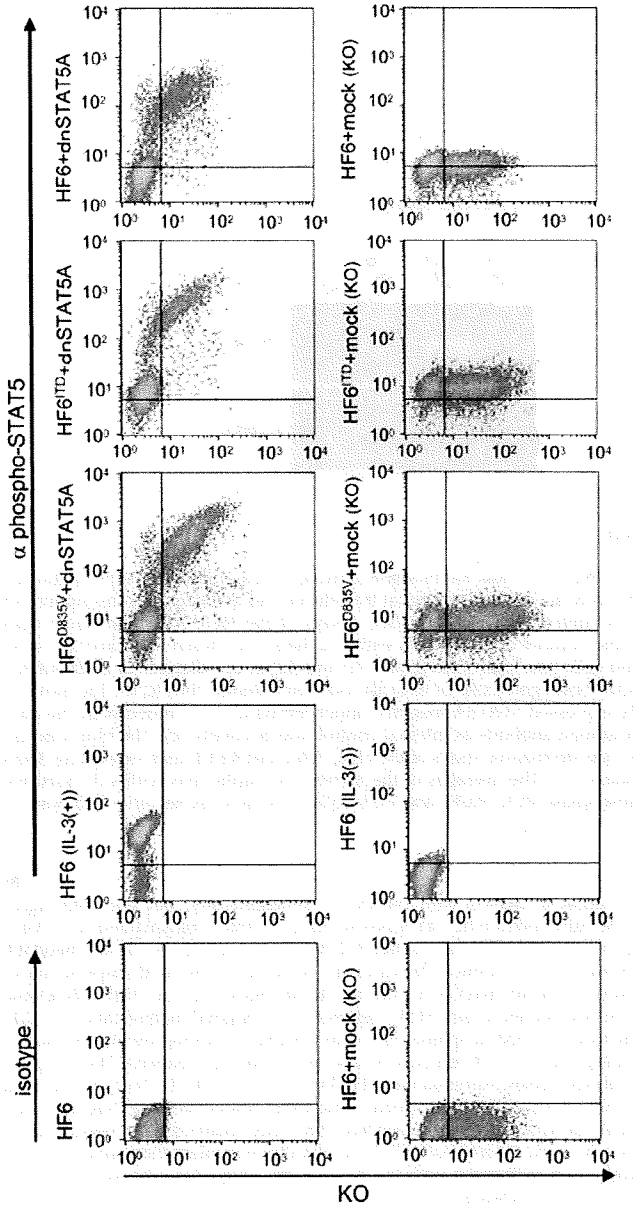
b
α phospho-STAT5
HF6+dnSTAT5A
HF6+mock (KO)
HF6ITD+dnSTAT5A
HF6ITD+mock (KO)
HF6D835V+dnSTAT5A
HF6D835V+mock (KO)
HF6 (IL-3(+))
HF6 (IL-3(-))
isotype
HF6
HF6+mock (KO)
KO

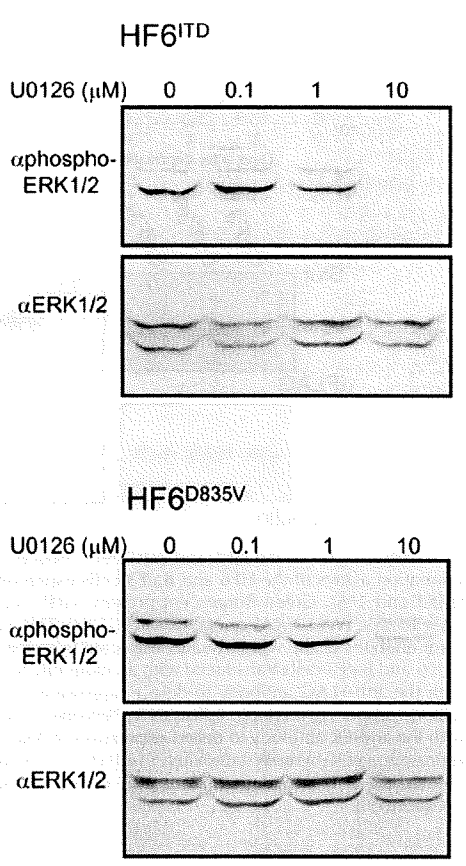
d
HF6ITD
U0126 (μM) 0 0.1 1 10
αphospho-ERK1/2
αERK1/2
HF6D835V
U0126 (μM) 0 0.1 1 10
αphospho-ERK1/2
αERK1/2

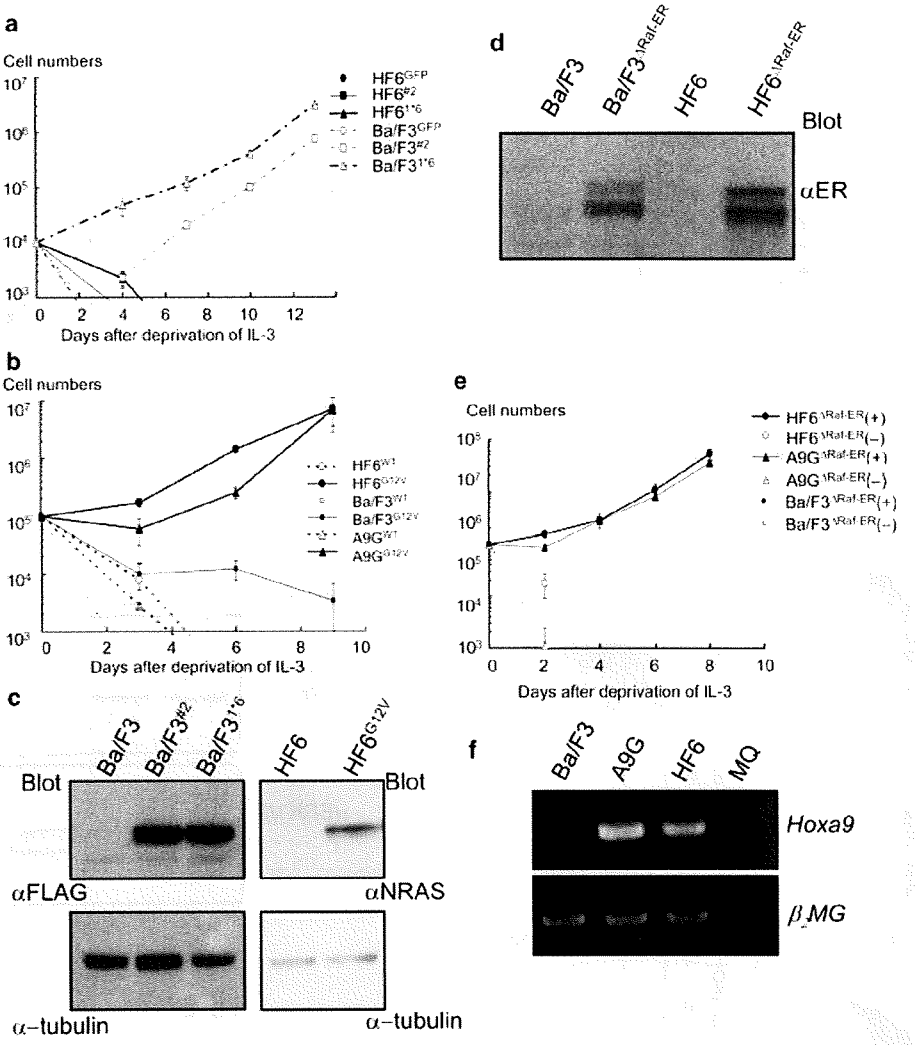

Figure 3 Transformation of the HF6 and A9G cells induced by direct activation of Ras/Raf/mitogen-activated protein kinase (MAPK) pathway. (**a**) Transformation assays of the HF6 and Ba/F3 cells expressing constitutively active forms of signal transducer and activator of transcription 5A (STAT5A) (#2 and 1*6). Green fluorescent protein (GFP) was used as a control. (**b**) Transformation assays of the HF6, A9G and Ba/F3 cells expressing wild-type (WT) *NRAS* or $NRAS^{G12V}$ (G12V). The averages of the number of viable cells with s.d. (bars) are shown in (**a**) and (**b**). (**c**, **d**) Western blot analyses of the whole lysates extracted from the transduced cells (see legends to panels (a) and (b)) in the absence of interleukin-3 (IL-3). (**c**) HF6 and Ba/F3 cells transduced with an inducible form of Raf (Δ*Raf*-estrogen receptor (ER)) (**d**) and their parental cells (**c**, **d**). The blot was probed with the anti-FLAG antibody to detect expression of ectopically expressed STAT5A mutants (upper left panel), or probed with the anti-*NRAS* antibody (upper right panel), followed by reprobe with the anti-α-tubulin antibody as internal control (lower panels) (**c**). The blot was also probed with the anti-ER antibody to detect expression of Δ*Raf*-ER (**d**). (**e**) Transformation assays of the HF6, A9G and Ba/F3 cells expressing Δ*Raf*-ER in the presence of 4-hydroxy-tamoxifen (4-OHT) (+) or vehicle control (−). The averages of the number of viable cells with s.d. (bars) are shown. (**f**) Analysis of *Hoxa9* transcripts in A9G cells using reverse transcriptase-PCR. Ba/F3 and HF6 cells were used as negative and positive controls, respectively.

Figure 4 Leukemogenesis induced by *mixed-lineage-leukemia* (*MLL*)-septin 6 (*SEPT6*) with $NRAS^{G12V}$ synergistically, but not with signal transducer and activator of transcription 5A (STAT5A)#2, *in vivo* under lethal conditioning. (**a**) Survival curves of mice transplanted with *MLL-SEPT6* and $NRAS^{G12V}$ (MS6/G12V; $n=6$), MS6 and *STAT5A*#2 (MS6/#2; $n=6$), MS6/GFP ($n=6$), neo/G12V ($n=6$), neo/#2 ($n=3$) and neo/GFP ($n=3$). (**b**) Representative macroscopic images of spleens obtained from each group of mice shown in (**a**). Scale bar 1 cm. (**c**, **d**) Representative histopathological analysis of morbid mice transplanted with MS6/#2, MS6/G12V (**c**, **d**), neo/G12V, and neo/#2 (**d**). Bone marrow (BM) cells (**c**) and paraffin sections of spleen (**d**) were stained with Wright-Giemsa and hematoxylin and eosin (H&E), respectively. Original magnification, ×200 (**c**) and ×40 (**d**); scale bars, 30 μm (c) and 200 μm (**d**). (**e**, **f**) Immunophenotype of BM or splenic (Sp) cells obtained from representative morbid mice transplanted with MS6/#2 (**e**, left panels), MS6/G12V (**e**, right panels), neo/G12V (**f**, left panels) and neo/#2 (**f**, right panels). The dot plots show each surface antigen labeled with a corresponding monoclonal antibody versus expression of GFP. Ly5.1, Gr-1, CD11b, Ter119, and c-Kit were labeled with phycoerythrin (PE)-conjugated and allophycocyanin (APC)-conjugated monoclonal antibodies, respectively. (**g**) Southern blot analysis to detect clonality (left panel) and proviral integration (right panel). Genomic DNA extracted from BM cells obtained from representative mice transplanted with MS6/G12V (lanes 4, 5, 9 and 10), MS6/GFP (lanes 2, 3, 7 and 8) and neo/GFP (5 months after transplantation; lanes 1 and 6) was digested with *Bam*HI (lanes 1–5) and *Nhe*I (lanes 6–10), respectively, and hybridized with the Neo probe. Oligoclonal bands of proviral integration and single bands of the proviral DNA are indicated by arrows and arrowheads, respectively.

($A9G^{\Delta Raf-ER}$) cells grew without IL-3 only in the presence of 4-hydroxy-tamoxifen (Figure 3e). Expression level of *Hoxa9* in A9G cells was shown in comparison with those in Ba/F3 and HF6 (negative and positive controls, respectively) cells by reverse transcriptase-PCR (Figure 3f).

Taken together, these results *in vitro* suggested the essential role of activation of the Ras/Raf/MAPK cascade together with *Hoxa9* upregulated by *MLL* fusion proteins in the transformation of the cells expressing *MLL* fusion protein.

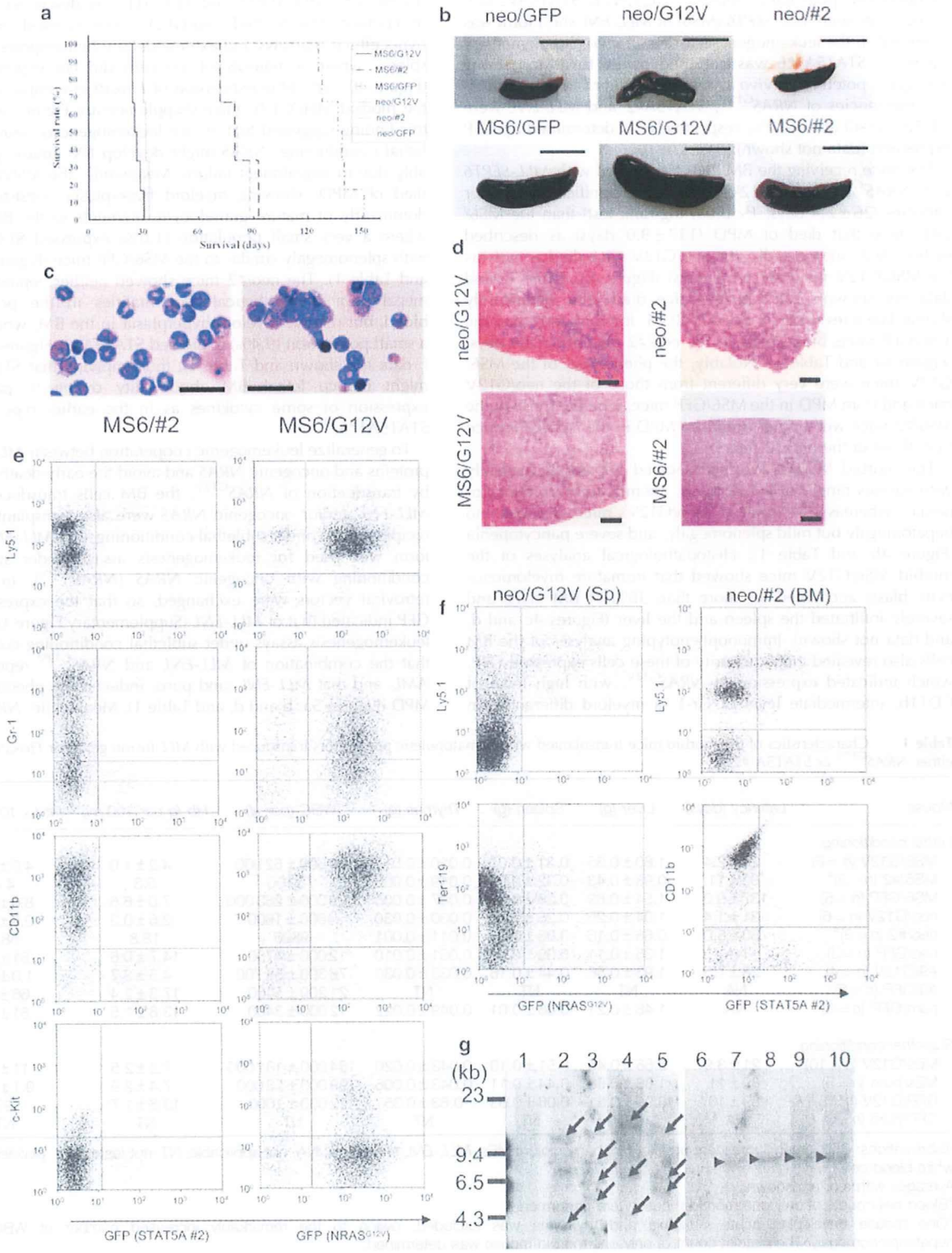

MLL *fusion proteins and oncogenic* NRAS *cooperate to induce acute leukemia, at least partly through aberrant expression of* Hoxa9

The findings on the transformation of HF6 cells *in vitro* led to the hypothesis that *MLL* fusion proteins might cooperate with activation of Ras to induce *AML in vivo*. To test this hypothesis, the oncogenic potential of $NRAS^{G12V}$ (G12V) or STAT5A#2 (#2) to cooperate with *MLL-SEPT6* (MS6) or *MLL-ENL* short form was examined in the leukemogenesis assays *in vivo* (Supplementary Figure 1). STAT5A1*6 was not used owing to its too strong oncogenic potential *in vivo* as reported earlier.[36] The transduction efficiencies of $NRAS^{G12V}$, STAT5A#2 and *MLL-ENL* were 30–50, 20–40 and 5–10%, respectively, as determined by GFP expression (data not shown).

The mice receiving the BM cells transduced with *MLL-SEPT6* and $NRAS^{G12V}$ (MS6/G12V) died with significantly shorter latencies (26 ± 2.4 days; $P<0.05$, log-rank test) than the MS6/GFP mice that died of MPD (137 ± 9.0 days) as described earlier,[6] but, unexpectedly, the neo/G12V mice died as early as the MS6/G12V mice (31 ± 1.4 days) (Figure 4a, Table 1, and data not shown). The MS6/#2 mice died with significantly shorter latencies (82 ± 11 days; $P<0.05$, log-rank test) than the MS6/GFP mice, but as early as the neo/#2 mice (80 ± 8.0 days) (Figure 4a and Table 1). Notably, the phenotypes of the MS6/G12V mice were very different from those of the neo/G12V mice and from MPD in the MS6/GFP mice, whereas those of the MS6/#2 mice were rather similar to MPD in the MS6/GFP mice than those of the neo/#2 mice.

The morbid MS6/G12V mice showed hepatosplenomegaly with various ranges of leukocytosis, anemia and thrombocytopenia, whereas the morbid neo/G12V mice showed no hepatomegaly but mild splenomegaly, and severe pancytopenia (Figure 4b and Table 1). Histopathological analyses of the morbid MS6/G12V mice showed that immature myelomonocytic blasts accounted for more than 30% of BM cells, and severely infiltrated the spleen and the liver (Figures 4c and d, and data not shown). Immunophenotyping analyses of the BM cells also revealed that a majority of these cells expressed GFP, which indicated expression of $NRAS^{G12V}$, with high level of CD11b, intermediate level of Gr-1 (a myeloid differentiation marker also known as Ly-6G) and low level of c-Kit (CD117, the receptor of stem cell factor) (Figure 4e). In addition, Southern blot analysis of genomic DNAs derived from the spleens of the MS6/G12V mice showed oligoclonal bands of proviral integration (Figure 4g). These results indicated that the MS6/G12V mice developed *AML* similar to the mice receiving BM cells transduced with *MLL-SEPT6* and *FLT3*-ITD, as described earlier.[6] In contrast, the morbid neo/G12V mice showed extremely hypocellular marrows and extramedullary hematopoiesis in the spleen, where a majority of the cells did not express Ly5.1 (Figure 4f), with little expression of *Hoxa9* in comparison with the morbid MS6/G12V mice (Supplementary Figure 3a). Thus, this finding suggested that, in our leukemogenesis assays under lethal conditioning, *NRAS* might develop BM aplasia presumably due to engraftment failure. Meanwhile, the MS6/#2 mice died of MPD, showing myeloid hyperplasia consisting predominantly of mature granulocytic elements in the BM cells, where a very small population (1.0%) expressed STAT5A#2, with splenomegaly similar to the MS6/GFP mice (Figures 4b–d, and Table 1). The neo/#2 mice showed neither hepatosplenomegaly nor hematological abnormalities in the peripheral blood, but relative myeloid hyperplasia in the BM, where only a small population (9.4%) expressed STAT5A#2 (Figures 4b and f, data not shown and Table 1), thus implying that STAT5A#2 might induce lethal BM abnormality owing to paracrine expression of some cytokines as in the earlier report using STAT5A1*6.[36]

To generalize leukemogenic cooperation between *MLL* fusion proteins and oncogenic *NRAS* and avoid the early death caused by transduction of $NRAS^{G12V}$, the BM cells transduced with *MLL-ENL* and/or oncogenic *NRAS* were also transplanted into recipient mice under sublethal conditioning. The *MLL-ENL* short form was used for leukemogenesis assays under sublethal conditioning with oncogenic *NRAS* ($NRAS^{G12V}$), in which retroviral vectors were exchanged, so that the expression of GFP indicated that of *MLL-ENL* (Supplementary Figure 1). These leukemogenesis assays under sublethal conditioning confirmed that the combination of *MLL-ENL* and $NRAS^{G12V}$ reproduced *AML*, and that *MLL-ENL* (and puro) induced the phenotype of MPD (Figures 5a, b and d, and Table 1). Meanwhile, $NRAS^{G12V}$

Table 1 Characteristics of the morbid mice transplanted with hematopoietic progenitors transduced with *MLL* fusion genes or *Hoxa9*, and/or either $NRAS^{G12V}$ or STAT5A #2

Mouse	*Latency (days)*	*Liver (g)*	*Spleen (g)*	*Thymus (g)*	*WBC (per μl)*	*Hb (g per 100 ml)*	*Plt (× 10^4 per μl)*
Lethal conditioning							
MS6/G12V ($n=6$)	26 ± 2.4	1.60 ± 0.35	0.31 ± 0.07	0.020 ± 0.012	74 600 ± 62 900	4.2 ± 1.0	4.0 ± 3.9
MS6/#2 ($n=3$)[a]	82 ± 11	0.98 ± 0.43	0.32 ± 0.03	0.019 ± 0.006	73 100	5.3	4.4
MS6/GFP ($n=6$)	137 ± 9.0	1.54 ± 0.69	0.26 ± 0.09	0.037 ± 0.005	309 000 ± 263 000	7.0 ± 6.6	8.0 ± 5.7
neo/G12V ($n=6$)	31 ± 1.4	1.04 ± 0.25	0.25 ± 0.08	0.030 ± 0.030	4600 ± 1800	2.5 ± 0.3	0.5 ± 0.4
neo/#2 ($n=3$)[a]	80 ± 8.0	0.66 ± 0.16	0.08 ± 0.06	0.011 ± 0.001	9800	18.8	58.2
neo/GFP ($n=3$)	NA	1.36 ± 0.11	0.09 ± 0.01	0.051 ± 0.010	12 000 ± 4700	14.7 ± 0.6	81 ± 13
A9/G12V ($n=4$)	28 ± 7.5	1.93 ± 0.56	0.44 ± 0.16	0.033 ± 0.030	76 300 ± 56 700	4.5 ± 2.7	1.0 ± 0.6
A9/GFP ($n=6$)	NA	NT	NT	NT	21 200 ± 5400	17.3 ± 2.4	66 ± 4.7
puro/GFP ($n=3$)	NA	1.48 ± 0.21	0.06 ± 0.01	0.049 ± 0.022	12 000 ± 3400	13.6 ± 1.5	81 ± 19
Sublethal conditioning							
MEs/G12V ($n=10$)	21 ± 3.9	2.56 ± 0.45	0.51 ± 0.10	0.043 ± 0.020	164 000 ± 131 000	7.2 ± 2.5	11 ± 4.5
MEs/puro ($n=5$)	89 ± 11	1.89 ± 0.58	0.44 ± 0.11	0.043 ± 0.006	99 000 ± 53 000	7.4 ± 2.9	9.1 ± 3.1
GFP/G12V ($n=5$)[b]	89 ± 10	0.90 ± 0.31	0.06 ± 0.03	0.63 ± 0.35	22 000 ± 1000	13.6 ± 1.7	97
GFP/puro ($n=3$)	NA	NT	NT	NT	NT	NT	NT

Abbreviations: GFP, green fluorescent protein; Hb, hemoglobin; MEs, *MLL-ENL* short form; NA, not applicable; NT, not tested; Plt, platelet; WBC, white blood cell.
Averages with s.d. are shown.
[a]Blood cell counts of only one morbid mouse were performed.
[b]One mouse developing acute leukemia and thymoma was excluded, owing to the remarkably increased number of WBCs and hepatosplenomegaly. The platelet count of only one morbid mouse was determined.

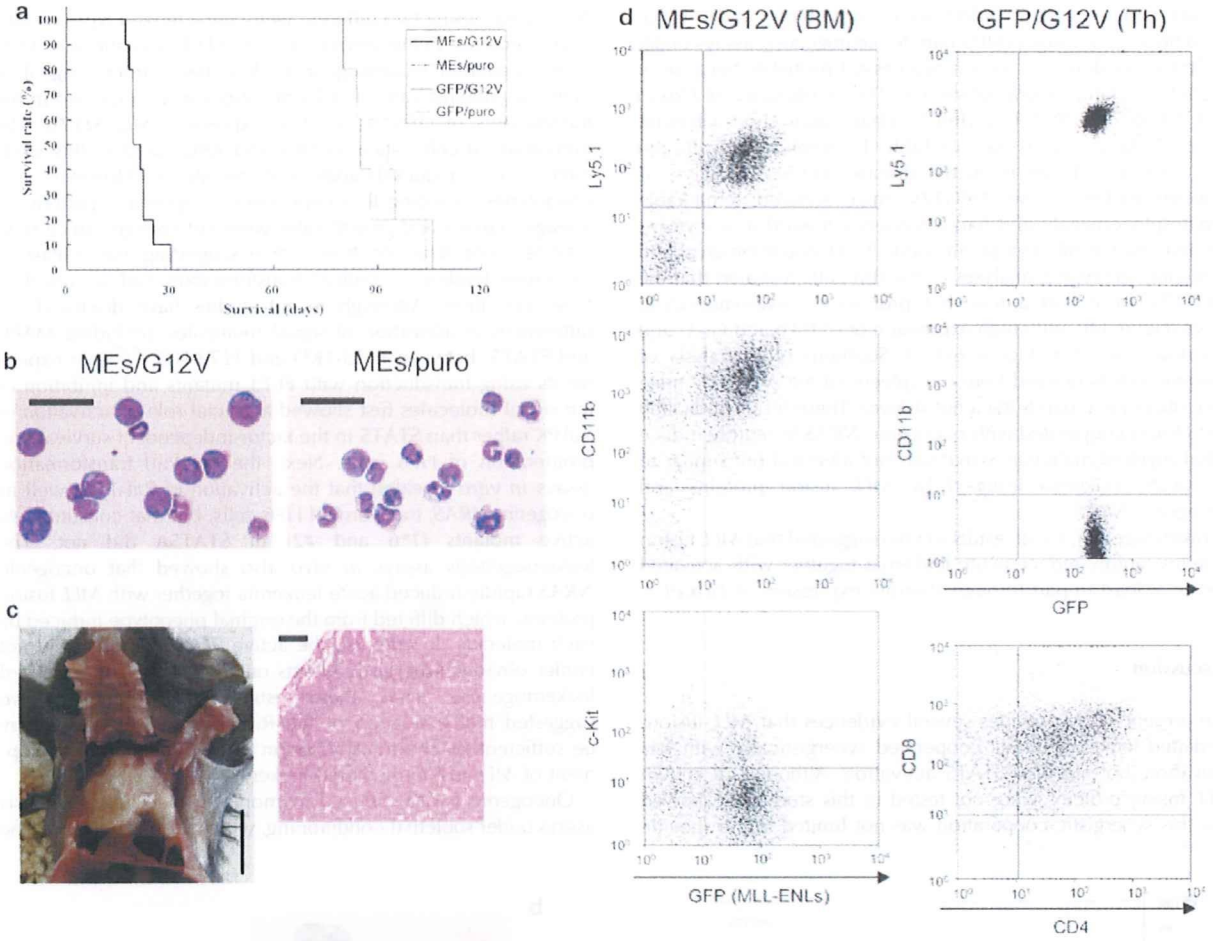

Figure 5 Leukemogenesis assays under sublethal conditioning using *mixed-lineage-leukemia/eleven nineteen leukemia* (*MLL-ENL*) and $NRAS^{G12V}$. (**a**) Survival curves of mice transplanted with a short form of *MLL-ENL* (MEs) and $NRAS^{G12V}$ (MEs/G12V) ($n=10$), MEs/puro ($n=5$), GFP/G12V ($n=5$) and green fluorescent protein (GFP)/puro ($n=3$). (**b**) Representative cytospin preparations of bone marrow (BM) cells obtained from morbid MEs/G12V and MEs/puro mice. The cells were stained with Wright-Giemsa. Original magnification 200×; Scale bars 30 μm. (**c**) Representative histopathologic images of thymus obtained from the GFP/G12V mouse. A paraffin section of the thymus was stained with hematoxylin and eosin (H&E). Original magnification, ×40; vertical and horizontal scale bars, 1 cm and 200 μm, respectively. (**d**) Immunophenotype of BM and thymic (Th) cells obtained from representative morbid MEs/G12V and GFP/G12V mice. The dot plots show each surface antigen labeled with a corresponding monoclonal antibody versus expression of GFP or CD4. Ly5.1, CD11b, CD4, and c-Kit and CD8 were labeled with phycoerythrin (PE)-conjugated and allophycocyanin (APC)-conjugated monoclonal antibodies, respectively.

(and GFP) led to thymoma, sometimes together with leukocytosis, with a long latency (Figures 5a, c and d, and Table 1). In addition, to examine the possibility that the phenotypes associated with STAT5A#2 might change, similar to oncogenic *NRAS*, the BM cells transduced with STAT5A#2 (in pMYs-IRES-EGFP) and/or *MLL-SEPT6* (in pMXs-neo) were again transplanted into recipient mice under sublethal conditioning. Within an observation period of 160 days, two of three neo/#2 mice under sublethal conditioning died with longer latencies (134 and 139 days) and showed the same phenotype of myeloid hyperplasia in the BM, where a small population (15%) expressed STAT5A#2, although these had different phenotypes of pancytopenia and splenomegaly (Supplementary Figure 3b and data not shown). In contrast, two of three MS6/#2 mice and all of the three MS6/GFP mice survived and showed no hematological abnormalities in the peripheral blood, whereas one of the MS6/#2 mice died (125 day) but could not be analyzed because of post-mortem change, within the observation period. Histopathological analysis of one MS6/#2 mouse, which was killed 150 days after the transplantation, showed no significant hepatosplenomegaly but mild myeloid hyperplasia in the BM (data not shown). Only 30% of the BM cells were positive for donor-derived Ly-5.1, and 7% of the BM cells were positive for GFP, indicating expression of STAT5A#2 (Supplementary Figure 3c), whereas reverse transcriptase-PCR analysis of the BM cells gave very weak signals of *MLL-SEPT6* after 30 cycles (data not shown), but clearly visible signals after 35 cycles (Supplementary Figure 3c). Therefore, sublethal conditioning seemed to be inappropriate for leukemogenesis assays using oncogenes, such as *MLL-SEPT6* and STAT5A#2, which had relatively weak oncogenic potential in comparison with *MLL-ENL* and $NRAS^{G12V}$.

Finally, we examined whether *Hoxa9* may be involved in cooperation between the *MLL* fusion protein and oncogenic *NRAS in vivo*, such as in transformation assays *in vitro*. The leukemogenesis assays using the BM cells transduced with

Hoxa9 and oncogenic *NRAS* were carried out under lethal conditioning, because preliminary leukemogenesis assays under sublethal conditioning were unsuccessful probably because of engraftment failure (data not shown). The combination of *Hoxa9* and *NRAS*^{G12V} (A9/G12V) led to death with short latencies (28 ± 7.5 days) (Figure 6a and Table 1), whereas *Hoxa9* (and GFP) *per se* induced no lethal disease within 120 days, as reported earlier.[37] The A9/G12V mice showed remarkable hepatosplenomegaly and had a tendency toward leukocytosis, anemia and thrombocytopenia (Table 1). Histopathological and immunophenotyping analyses of the BM cells revealed that the A9/G12V mice had a few, but prominent, myelomonocytic blasts (Figure 6b), with high expression of CD11b and Gr-1, and low level of c-Kit (Figure 6c). A Southern blot analysis of genomic DNAs derived from the spleens of the A9/G12V mice gave oligoclonal bands (data not shown). These results indicated that *Hoxa9* cooperated with oncogenic *NRAS* to rapidly induce lethal myeloid malignancy that was not identical but similar to the acute leukemia induced by *MLL* fusion proteins and oncogenic *NRAS*.

Taken together, these results *in vivo* suggested that *MLL* fusion proteins rapidly induce acute leukemia together with activated *NRAS*, at least in part through aberrant expression of *Hoxa9*.

Discussion

The present study provides several evidences that *MLL*-fusion-mediated leukemogenesis cooperated synergistically with Ras activation, but not with STAT5 activation. Although all known *MLL* fusion proteins were not tested in this study, we showed that this synergistic cooperation was not limited to the specific *MLL* fusion, using two different well-characterized types of *MLL* fusion proteins. In the light of the role of FLT3 mutations in *MLL*-fusion-mediated leukemogenesis described earlier,[6] signaling pathways downstream of FLT3 mutations were analyzed in the transfectants of HF6, a cell line expressing *MLL-SEPT6*. The immortalized cells, such as HF6 and A9G, used in this study might have acquired additional mutations. However, the phenotypes including IL-3 dependency, expression patterns of lineage markers and growth rates were not changed since their establishment (data not shown), thus suggesting that at least no mutations leading to critical transformation had occurred in these cell lines. Although recent studies have disclosed the differences in activation of signal molecules, including MAPK and STAT5, between *FLT3*-TKD and *FLT3*-ITD,[24,38] our experiments using transduction with FLT3 mutants and inhibition of the signal molecules first showed a crucial role of activation of MAPK rather than STAT5 in the factor-independent survival and proliferation of HF6 cells. Next, the myeloid transformation assays *in vitro* revealed that the activation of Raf-1, as well as oncogenic *NRAS*, transformed HF6 cells, but that constitutively active mutants (1*6 and #2) of STAT5A did not. The leukemogenesis assays *in vivo* also showed that oncogenic *NRAS* rapidly induced acute leukemia together with *MLL* fusion proteins, which differed from the original phenotype induced by each molecule. In contrast, the active STAT5A mutant did not confer obvious synergistic effects on the *MLL*-fusion-mediated leukemogenesis. Thus, these results *in vitro* and *in vivo* suggested that activation of the Ras/Raf/MAPK pathway may be sufficient for the transformation of HF6 cells and development of *MLL*-fusion-mediated leukemia.

Oncogenic *NRAS* induced thymoma in the leukemogenesis assays under sublethal conditioning, which is consistent with the

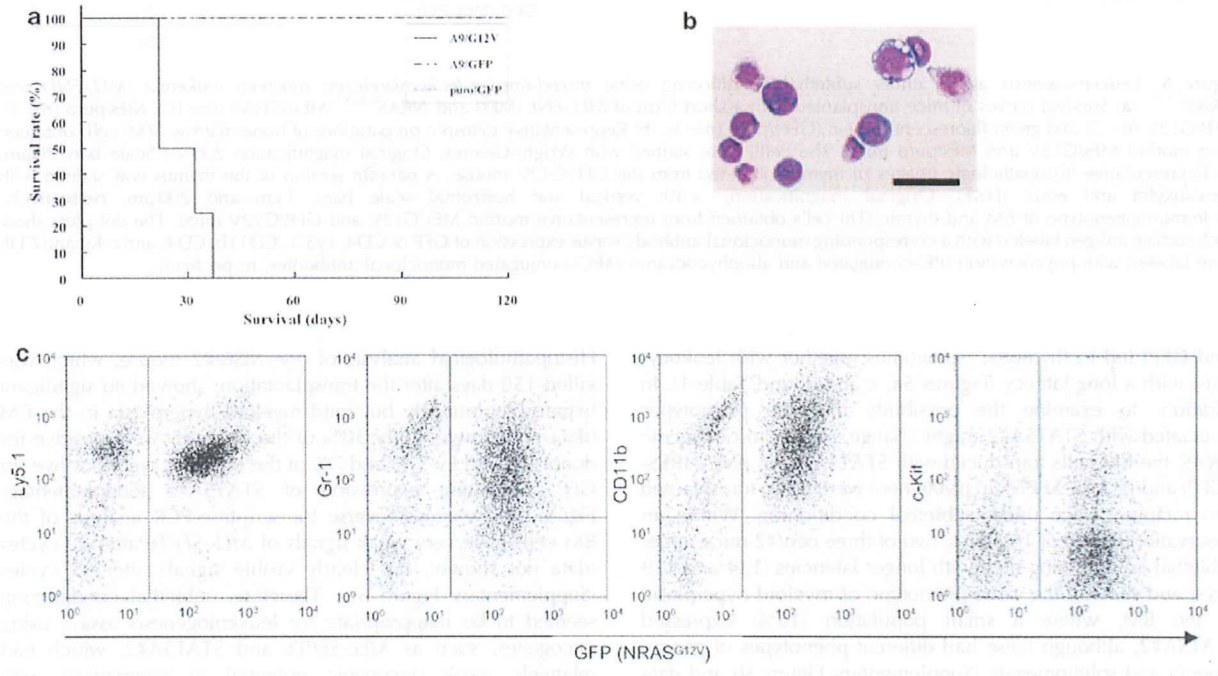

Figure 6 Leukemogenesis induced by *Hoxa9* and oncogenic neuroblastoma RAS viral (v-ras) oncogene homolog (*NRAS*) under lethal conditioning. (**a**) Survival curves of mice transplanted with *Hoxa9* and *NRAS*^{G12V} (A9/G12V; $n = 4$), A9/green fluorescent protein (GFP) ($n = 6$) and puro/GFP ($n = 3$). (**b**) Representative cytospin preparations of bone marrow (BM) cells obtained from morbid A9/G12V mice. The cells were stained with Wright-Giemsa. Original magnification, × 200; scale bar, 30 μm. (**c**) Immunophenotype of BM cells obtained from representative morbid A9/G12V mice. The dot plots show each surface antigen labeled with a corresponding monoclonal antibody versus expression of GFP. Ly5.1, Gr-1, CD11b, and c-Kit were labeled with phycoerythrin (PE)-conjugated and allophycocyanin (APC)-conjugated monoclonal antibodies, respectively.

development of T-lymphoma by *FLT3*-TKD in our experimental system (Ono *et al.*, unpublished data), whereas it led to the development of BM aplasia in our leukemogenesis assays under lethal conditioning. This difference in the disease phenotypes implies that forced expression of oncogenic *NRAS* in BM progenitors might be involved in its inhibitory effects on the engraftment of radioprotective cells as well as the antiproliferative effect of oncogenic *NRAS* in the early phase of the transplantation.[39] These disease phenotypes were also different from the development of MPD in the earlier reports.[39,40] This discrepancy might be due to the differences in the experimental systems, such as the retroviral transduction and mice strains. Meanwhile, the BM progenitors transduced with *Hoxa9* and $NRAS^{G12V}$ seemed to result in engraftment failure under sublethal conditioning, but these rapidly developed myeloid malignancy under lethal conditioning. A recent study using BM transplantation showed the possibility of drastic fluctuation in the engraftment of donor cells receiving pathological modification under sublethal conditioning;[41] hence, our unsuccessful results under sublethal conditioning might be associated with some instability of the transplantation.

Our leukemogenesis assays showed a definitively synergistic cooperation between *MLL* fusion proteins and oncogenic *NRAS* in the acceleration of disease onset and change of the phenotypes. Interestingly, the synergistic cooperation between *MLL* fusion proteins and Ras/Raf/MAPK activation closely correlated with recent clinical studies reporting the frequent coincidence of *MLL* fusion genes and mutations of *RAS*[20] or *RAF*.[42] It was reported that the additional expression of oncogenic *KRAS* induced an acute promyelocytic leukemia-like disease in transgenic mice expressing promyelocytic leukemia/retinoic acid receptor-α with an increased penetrance and decreased latency, although neither the penetrance nor the latency was significantly different from those in mice that died of MPD by expression of oncogenic *KRAS* alone.[43] Other groups recently reported that the combination of oncogenic *NRAS* and *MLL-AF9*[44] or *MLL-ENL*[45] is capable of developing *AML*, and that induced repression of oncogenic *NRAS* on the combination reverted *AML* to MPD by the *MLL* fusion gene (*MLL-AF9*) alone.[44] Although our findings that *MLL* fusion proteins and oncogenic *NRAS* cooperate to induce *AML* confirmed these notions, the present study further analyzed the involvement of *Hoxa9* and Raf, downstream of the cooperation between *MLL* fusion proteins and oncogenic *NRAS*. The myeloid transformation assays *in vitro* showed that the activation of Raf-1, as well as oncogenic *NRAS*, transformed A9G, a cell line expressing *Hoxa9*. The leukemogenesis assays *in vivo* also showed that *Hoxa9* and oncogenic *NRAS* rapidly developed myeloid malignancy. These results *in vitro* and *in vivo* suggested that, as downstream molecules, *Hoxa9* and Raf may have important roles in the synergistic leukemogenesis by *MLL* fusion proteins and oncogenic *NRAS*.

Our findings suggest a possible model of *MLL*-fusion-mediated leukemogenesis that was essentially recapitulated by *Hoxa9* expression and Ras/Raf/MAPK activation (Figure 7). In the context of secondary genetic alterations, such as *FLT3* mutations, this model explains the clinical features of acute leukemia with 11q23 translocations. First, overexpression, as well as TKD mutations, of *FLT3* frequently detected in the *MLL*-rearranged infant acute leukemia may be involved in the leukemogenesis mainly through activation of Ras/Raf/MAPK, because several studies reported that the signaling pathway of wild-type *FLT3* is similar to *FLT3*-TKD rather than *FLT3*-ITD.[24,38] Second, besides *FLT3*, other unknown molecular pathways that lead to the activation of Ras/Raf/MAPK might also be involved in

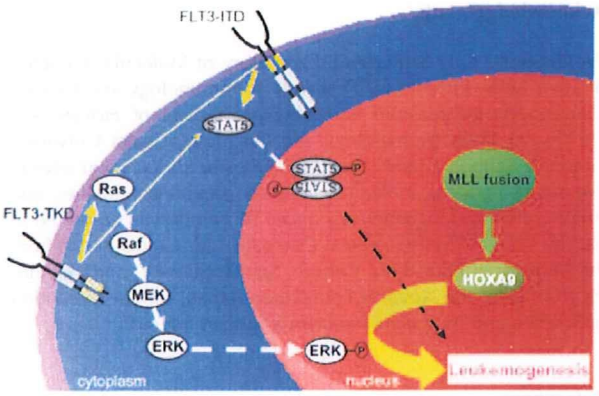

Figure 7 A model of *mixed-lineage-leukemia* (*MLL*)-mediated leukemogenesis together with secondary genetic alterations. *MLL* fusion protein and secondary genetic alterations cooperate to induce acute leukemia through synergistic molecular crosstalk between aberrant expression of *Hox* genes, including *Hoxa9*, and the activation of Ras/Raf/mitogen-activated protein kinase (MAPK). Other signaling pathways, including signal transducer and activator of transcription 5 (STAT5) activation, only additively affect the leukemogenic potential.

the *MLL*-rearranged leukemia carrying no known genetic alterations, as *FLT3* alterations are not found very frequently in most *MLL*-rearranged leukemia except in infants.[46,47] Meanwhile, in the context of *MLL* fusion proteins, we analyzed the role of the *Hoxa9*-mediated pathway leading to leukemogenesis. Recent studies revealed that one of the *Hox*-cofactor molecules, *Meis1*, is an essential molecule involved in normal hematopoiesis[48] as well as *Hoxa9*-mediated leukemogenesis.[49] However, our experimental system[6] using BM cells transduced with *MLL* fusion proteins did not detect any significant upregulation of *Meis1* in comparison with the mock transduction as reported earlier,[50] in contrast with the findings by other groups.[14] Therefore, we focused on *Hoxa9*, one of the key molecules directly upregulated by *MLL* fusion proteins. Interestingly, a recent study showed that the combination of *Hoxa9* and *Meis1* cooperated with *Trib1*, which enhanced the phosphorylation of ERK, to induce acute leukemia in the BM transplantation assays.[51] Their study is not inconsistent with our findings; thus, the *HOX* and Ras/Raf/MAPK axes may have central roles in the molecular network of *MLL*-mediated leukemogenesis, which might be additively affected by other pathways, such as activation of STAT5 (Figure 7). In addition, at least, endogenous expression of *Meis1* in A9G cells is also considered to be important in this network, but further analysis will be required to clarify the role of *Meis1* in the collaboration between *HOX* and MAPK axes.

Conclusion

This study suggests that *MLL* fusion proteins synergistically cooperate with Ras/Raf/MAPK activation in leukemogenesis, at least partly through the upregulation of *Hoxa9*. Future studies analyzing the molecular crosstalk between *Hoxa9* and the Ras/Raf/MAPK cascade are expected to provide novel insights into the molecular mechanism of *MLL*-fusion-mediated leukemogenesis.

Conflict of interest

The authors declare no conflict of interest.

Acknowledgements

We thank Dr Guy Sauvageau (Laboratory of Molecular Genetics of Stem Cells, Institute for Research in Immunology and Cancer, Canada) for the plasmid harboring a fragment of *Hoxa9*, and Dr Yusuke Satoh (Hematology and Oncology, Osaka University Graduate School of Medicine, Osaka, Japan) for technical advice. We are also grateful to R&D Systems for providing cytokines, and Brian Quinn for language assistance. This work was supported in part by Chugai Pharmaceutical Company Ltd, Grants-in-Aid from the Ministry of Education, Culture, Sports, Science, and Technology in Japan, the Novartis Foundation (Japan) for the Promotion of Science and the Japan Leukaemia Research Fund.

References

1 Vogelstein B, Kinzler KW. Cancer genes and the pathways they control. *Nat Med* 2004; **10**: 789–799.
2 Look AT. Oncogenic transcription factors in the human acute leukemias. *Science* 1997; **278**: 1059–1064.
3 Rowley JD. The critical role of chromosome translocations in human leukemias. *Annu Rev Genet* 1998; **32**: 495–519.
4 Gilliland DG, Tallman MS. Focus on acute leukemias. *Cancer Cell* 2002; **1**: 417–420.
5 Kelly LM, Kutok JL, Williams IR, Boulton CL, Amaral SM, Curley DP *et al.* PML/RARalpha and FLT3-ITD induce an APL-like disease in a mouse model. *Proc Natl Acad Sci USA* 2002; **99**: 8283–8288.
6 Ono R, Nakajima H, Ozaki K, Kumagai H, Kawashima T, Taki T *et al.* Dimerization of MLL fusion proteins and FLT3 activation synergize to induce multiple-lineage leukemogenesis. *J Clin Invest* 2005; **115**: 919–929.
7 Schessl C, Rawat VP, Cusan M, Deshpande A, Kohl TM, Rosten PM *et al.* The *AML1-ETO* fusion gene and the FLT3 length mutation collaborate in inducing acute leukemia in mice. *J Clin Invest* 2005; **115**: 2159–2168.
8 Stubbs MC, Kim YM, Krivtsov AV, Wright RD, Feng Z, Agarwal J *et al.* MLL-AF9 and FLT3 cooperation in acute myelogenous leukemia: development of a model for rapid therapeutic assessment. *Leukemia* 2008; **22**: 66–77.
9 Watanabe-Okochi N, Kitaura J, Ono R, Harada H, Harada Y, Komeno Y *et al.* AML1 mutations induced MDS and MDS/AML in a mouse BMT model. *Blood* 2008; **111**: 4297–4308.
10 Ayton PM, Cleary ML. Molecular mechanisms of leukemogenesis mediated by MLL fusion proteins. *Oncogene* 2001; **20**: 5695–5707.
11 Meyer C, Kowarz E, Hofmann J, Renneville A, Zuna J, Trka J *et al.* New insights to the MLL recombinome of acute leukemias. *Leukemia* 2009; **23**: 1490–1499.
12 Yokoyama A, Somervaille TC, Smith KS, Rozenblatt-Rosen O, Meyerson M, Cleary ML. The menin tumor suppressor protein is an essential oncogenic cofactor for MLL-associated leukemogenesis. *Cell* 2005; **123**: 207–218.
13 Daser A, Rabbitts TH. Extending the repertoire of the *mixed-lineage leukemia* gene *MLL* in leukemogenesis. *Genes Dev* 2004; **18**: 965–974.
14 Hess JL. MLL: a histone methyltransferase disrupted in leukemia. *Trends Mol Med* 2004; **10**: 500–507.
15 Corral J, Lavenir I, Impey H, Warren AJ, Forster A, Larson TA *et al.* An *MLL-AF9* fusion gene made by homologous recombination causes acute leukemia in chimeric mice: a method to create fusion oncogenes. *Cell* 1996; **85**: 853–861.
16 Drynan LF, Pannell R, Forster A, Chan NM, Cano F, Daser A *et al.* MLL fusions generated by Cre-loxP-mediated *de novo* translocations can induce lineage reassignment in tumorigenesis. *EMBO J* 2005; **24**: 3136–3146.
17 Wang J, Iwasaki H, Krivtsov A, Febbo PG, Thorner AR, Ernst P *et al.* Conditional *MLL-CBP* targets GMP and models therapy-related myeloproliferative disease. *EMBO J* 2005; **24**: 368–381.
18 Chen W, Li Q, Hudson WA, Kumar A, Kirchhof N, Kersey JH. A murine *MLL-AF4* knock-in model results in lymphoid and myeloid deregulation and hematologic malignancy. *Blood* 2006; **108**: 669–677.
19 Taketani T, Taki T, Sugita K, Furuichi Y, Ishii E, Hanada R *et al.* FLT3 mutations in the activation loop of tyrosine kinase domain are frequently found in infant ALL with *MLL* rearrangements and pediatric ALL with hyperdiploidy. *Blood* 2004; **103**: 1085–1088.
20 Liang DC, Shih LY, Fu JF, Li HY, Wang HI, Hung IJ *et al.* K-Ras mutations and N-Ras mutations in childhood acute leukemias with or without mixed-lineage leukemia gene rearrangements. *Cancer* 2006; **106**: 950–956.
21 Gilliland DG, Griffin JD. The roles of FLT3 in hematopoiesis and leukemia. *Blood* 2002; **100**: 1532–1542.
22 Armstrong SA, Staunton JE, Silverman LB, Pieters R, den Boer ML, Minden MD *et al.* *MLL* translocations specify a distinct gene expression profile that distinguishes a unique leukemia. *Nat Genet* 2002; **30**: 41–47.
23 Murata K, Kumagai H, Kawashima T, Tamitsu K, Irie M, Nakajima H *et al.* Selective cytotoxic mechanism of GTP-14564, a novel tyrosine kinase inhibitor in leukemia cells expressing a constitutively active Fms-like tyrosine kinase 3 (FLT3). *J Biol Chem* 2003; **278**: 32892–32898.
24 Choudhary C, Schwable J, Brandts C, Tickenbrock L, Sargin B, Kindler T *et al.* AML-associated Flt3 kinase domain mutations show signal transduction differences compared with Flt3 ITD mutations. *Blood* 2005; **106**: 265–273.
25 Nosaka T, Kawashima T, Misawa K, Ikuta K, Mui AL, Kitamura T. STAT5 as a molecular regulator of proliferation, differentiation and apoptosis in hematopoietic cells. *EMBO J* 1999; **18**: 4754–4765.
26 Schubbert S, Shannon K, Bollag G. Hyperactive Ras in developmental disorders and cancer. *Nat Rev Cancer* 2007; **7**: 295–308.
27 Ariyoshi K, Nosaka T, Yamada K, Onishi M, Oka Y, Miyajima A *et al.* Constitutive activation of STAT5 by a point mutation in the SH2 domain. *J Biol Chem* 2000; **275**: 24407–24413.
28 Onishi M, Nosaka T, Misawa K, Mui AL, Gorman D, McMahon M *et al.* Identification and characterization of a constitutively active STAT5 mutant that promotes cell proliferation. *Mol Cell Biol* 1998; **18**: 3871–3879.
29 Kitamura T, Koshino Y, Shibata F, Oki T, Nakajima H, Nosaka T *et al.* Retrovirus-mediated gene transfer and expression cloning: powerful tools in functional genomics. *Exp Hematol* 2003; **31**: 1007–1014.
30 Kroon E, Krosl J, Thorsteinsdottir U, Baban S, Buchberg AM, Sauvageau G. Hoxa9 transforms primary bone marrow cells through specific collaboration with Meis1a but not Pbx1b. *EMBO J* 1998; **17**: 3714–3725.
31 Sakaue-Sawano A, Kurokawa H, Morimura T, Hanyu A, Hama H, Osawa H *et al.* Visualizing spatiotemporal dynamics of multicellular cell-cycle progression. *Cell* 2008; **132**: 487–498.
32 Calvo KR, Sykes DB, Pasillas M, Kamps MP. Hoxa9 immortalizes a granulocyte-macrophage colony-stimulating factor-dependent promyelocyte capable of biphenotypic differentiation to neutrophils or macrophages, independent of enforced meis expression. *Mol Cell Biol* 2000; **20**: 3274–3285.
33 Ono R, Ihara M, Nakajima H, Ozaki K, Kataoka-Fujiwara Y, Taki T *et al.* Disruption of *Sept6*, a fusion partner gene of *MLL*, does not affect ontogeny, leukemogenesis induced by *MLL-SEPT6*, or phenotype induced by the loss of *Sept4*. *Mol Cell Biol* 2005; **25**: 10965–10978.
34 Nosaka T, van Deursen JM, Tripp RA, Thierfelder WE, Witthuhn BA, McMickle AP *et al.* Defective lymphoid development in mice lacking Jak3. *Science* 1995; **270**: 800–802.
35 Moriggl R, Gouilleux-Gruart V, Jähne R, Berchtold S, Gartmann C, Liu X *et al.* Deletion of the carboxyl-terminal transactivation domain of MGF-STAT5 results in sustained DNA binding and a dominant negative phenotype. *Mol Cell Biol* 1996; **16**: 5691–5700.
36 Schwaller J, Parganas E, Wang D, Cain D, Aster JC, Williams IR *et al.* STAT5 is essential for the myelo- and lymphoproliferative disease induced by TEL/JAK2. *Mol Cell* 2000; **6**: 693–704.
37 Nakamura T, Largaespada DA, Shaughnessy Jr JD, Jenkins NA, Copeland NG. Cooperative activation of Hoxa and Pbx1-related genes in murine myeloid leukaemias. *Nat Genet* 1996; **12**: 149–153.
38 Grundler R, Miething C, Thiede C, Peschel C, Duyster J. FLT3-ITD and tyrosine kinase domain mutants induce 2 distinct phenotypes in a murine bone marrow transplantation model. *Blood* 2005; **105**: 4792–4799.

39 MacKenzie KL, Dolnikov A, Millington M, Shounan Y, Symonds G. Mutant N-ras induces myeloproliferative disorders and apoptosis in bone marrow repopulated mice. *Blood* 1999; **93**: 2043–2056.
40 Parikh C, Subrahmanyam R, Ren R. Oncogenic NRAS rapidly and efficiently induces CMML- and AML-like diseases in mice. *Blood* 2006; **108**: 2349–2357.
41 Santaguida M, Schepers K, King B, Sabnis AJ, Forsberg EC, Attema JL *et al.* JunB protects against myeloid malignancies by limiting hematopoietic stem cell proliferation and differentiation without affecting self-renewal. *Cancer Cell* 2009; **15**: 341–352.
42 Christiansen DH, Andersen MK, Desta F, Pedersen-Bjergaard J. Mutations of genes in the receptor tyrosine kinase (RTK)/RAS-BRAF signal transduction pathway in therapy-related myelodysplasia and acute myeloid leukemia. *Leukemia* 2005; **19**: 2232–2240.
43 Chan IT, Kutok JL, Williams IR, Cohen S, Moore S, Shigematsu H *et al.* Oncogenic K-ras cooperates with PML-RAR alpha to induce an acute promyelocytic leukemia-like disease. *Blood* 2006; **108**: 1708–1715.
44 Kim WI, Matise I, Diers MD, Largaespada DA. RAS oncogene suppression induces apoptosis followed by more differentiated and less myelosuppressive disease upon relapse of acute myeloid leukemia. *Blood* 2009; **113**: 1086–1096.
45 Zuber J, Radtke I, Pardee TS, Zhao Z, Rappaport AR, Luo W *et al.* Mouse models of human AML accurately predict chemotherapy response. *Genes Dev* 2009; **23**: 877–889.
46 Chillon MC, Fernandez C, Garcia-Sanz R, Balanzategui A, Ramos F, Fernandez-Calvo J *et al.* FLT3-activating mutations are associated with poor prognostic features in AML at diagnosis but they are not an independent prognostic factor. *Hematol J* 2004; **5**: 239–246.
47 Bacher U, Haferlach C, Kern W, Haferlach T, Schnittger S. Prognostic relevance of FLT3-TKD mutations in AML: the combination matters–an analysis of 3082 patients. *Blood* 2008; **111**: 2527–2537.
48 Hisa T, Spence SE, Rachel RA, Fujita M, Nakamura T, Ward JM *et al.* Hematopoietic, angiogenic and eye defects in Meis1 mutant animals. *EMBO J* 2004; **23**: 450–459.
49 Wong P, Iwasaki M, Somervaille TC, So CW, Cleary ML. Meis1 is an essential and rate-limiting regulator of MLL leukemia stem cell potential. *Genes Dev* 2007; **21**: 2762–2774.
50 Horton SJ, Grier DG, McGonigle GJ, Thompson A, Morrow M, De Silva I *et al.* Continuous MLL-ENL expression is necessary to establish a 'Hox Code' and maintain immortalization of hematopoietic progenitor cells. *Cancer Res* 2005; **65**: 9245–9252.
51 Jin G, Yamazaki Y, Takuwa M, Takahara T, Kaneko K, Kuwata T *et al.* Trib1 and Evi1 cooperate with Hoxa and Meis1 in myeloid leukemogenesis. *Blood* 2007; **109**: 3998–4005.

Supplementary Information accompanies the paper on the Leukemia website (http://www.nature.com/leu)

Journal of Pediatric Surgery (2009) 44, E31–E35

ELSEVIER

Journal of Pediatric Surgery

www.elsevier.com/locate/jpedsurg

Manifestation of alveolar rhabdomyosarcoma as primary cutaneous lesions in a neonate with Beckwith-Wiedemann syndrome

Minoru Kuroiwa [a,*], Jun Sakamoto [a], Akira Shimada [b], Norio Suzuki [a], Junko Hirato [c], Myoung-Ja Park [b], Manabu Sotomatsu [b], Yasuhide Hayashi [b]

[a] *Department of Surgery, Gunma Children's Medical Center, Shibukawa, Gunma 377-8577, Japan*
[b] *Department of Hematology/Oncology, Gunma Children's Medical Center, Shibukawa, Gunma 377-8577, Japan*
[c] *Department of Human Pathology, Graduate School of Medicine, Gunma University, Maebashi, Gunma 371-8511, Japan*

Received 16 July 2008; revised 3 December 2008; accepted 3 December 2008

Key words:
Beckwith-Wiedemann syndrome;
Alveolar rhabdomyosarcoma;
Blueberry muffin baby

Abstract We report a rare case of neonatal Beckwith-Wiedemann syndrome (BWS) associated with alveolar rhabdomyosarcoma (RMS). Alveolar RMS was diagnosed on the basis of excisional biopsy. Chemotherapy was initiated and followed by bone marrow transplantation. The patient, who is now 3 years and 11 months of age, is alive 46 months after the initial diagnosis, albeit with disease. We could not detect the *PAX3-FKHR* or *PAX7-FKHR* transcripts; however, we could observe hypomethylation of the differentially methylated region of the long QT intronic transcript 1. Thus, neonatal alveolar RMS with BWS may result from an alternate molecular pathway.

Beckwith-Wiedemann syndrome (BWS) [1] is a congenital overgrowth syndrome with 3 principal clinical features (omphalocele, macroglossia, and gigantism); BWS is also associated with various malignant tumors such as Wilms' tumor, hepatoblastoma, and rhabdomyosarcoma (RMS).

Only 10% of RMS cases are reported in the first year of life, and cases of neonatal RMS manifesting as a primary skin lesion are extremely rare [2]. Here, we report the case of a neonate suffering from BWS associated with RMS that manifested as a primary skin lesion.

* Corresponding author. Tel.: +81 279 52 3551; fax: +81 279 52 2045.
E-mail address: kuroiwa@gcmc.pref.gunma.jp (M. Kuroiwa).

0022-3468/$ – see front matter © 2009 Elsevier Inc. All rights reserved.
doi:10.1016/j.jpedsurg.2008.12.010

1. Case report

A 1-day-old newborn was referred to our hospital for the treatment of an omphalocele. The patient exhibited the clinical features of BWS (facial nevus flammeus, macroglossia, and gigantism). The omphalocele was treated successfully. However, at 15 days of age, small reddish nodules were observed on the extremities and chest of the patient. Subsequently, a number of small nodules appeared on the head, trunk, and buttock, indicative of the condition referred to as "blueberry muffin baby" (Fig. 1). Biopsy of the tumor revealed that it was arranged in the form of solid nests of undifferentiated cells, whereas the results of immunohistochemical studies on the tumor cells were positive for desmin, myogenin, myoD1, and myoglobin (Fig. 2). We diagnosed this condition as a case of alveolar RMS.

Fig. 1 Multiple cutaneous and subcutaneous lesions (a condition termed as blueberry muffin baby) in the patient at 28 days of age.

However, there was no evidence of a primary lesion in the magnetic resonance imaging scans. Chemotherapy, comprising vincristine, actinomycin D, and cyclophosphamide (VAC), was initiated. The multiple skin tumors disappeared after 5 courses of VAC, which was followed by 4 courses of modified ifosfamide-cisplatin-etoposide therapy and a bone marrow transplantation procedure.

Fluorescence in situ hybridization studies did not reveal any specific chromosomal translocations, and we could not detect *PAX3-FKHR* or *PAX7-FKHR* transcripts. However, Southern blotting analysis of the blood and tumor tissues demonstrated the demethylation of the differentially methylated regions in the long QT intronic transcript 1 (DMR-LIT1), a process that leads to the biallelic expression of the *KCNQ1* overlapping transcript 1 (*KCNQ1OT1*; the paternally expressed antisense transcript located in the *KCNQ1* gene at 11p15).

The findings from imaging studies conducted at 14 months of age revealed that the RMS was in complete remission. However, RMS recurrence along with lung metastasis was confirmed 2 months later. The patient was administered VAC and campothecin (CPT-11) for 12 months, which resulted in disappearance of the skin lesions. The patient underwent 6 months of follow-up (up to an age of 2 years and 9 months), after which RMS recurred again. However, the disease progression was controlled by administration of VAC and CPT-11. Rhabdomyosarcoma in the patient, who is now 3 years and 11 months of age, is now in remission, with no evidence of the disease in the results from imaging studies.

2. Discussion

Beckwith-Wiedemann syndrome is a genetically heterogeneous disorder, and its occurrence is known to be related to genetic abnormalities that affect insulin-like growth factor 2, H19, cyclin-dependent kinase inhibitor 1C, and *KCNQ1OT1* [3]. In particular, uniparental paternal disomy at chromosome 11p15 was observed in up to 20% of BWS patients; imprinting defects at *KCNQ1OT1*, in up to 50% patients [4,5]; and mutation in cyclin-dependent kinase inhibitor 1C, in up to 5% patients; and hypermethylation in H19, in up to 7% patients.

Beckwith-Wiedemann syndrome has also been known to increase the risk of malignancies; although the actual risk of malignancy in cases of BWS is estimated to be 7.5%, it increases to 10% in cases of coexisting hemihypertrophy [6]. The most common malignancy associated with BWS is Wilms' tumor, followed by adrenal cortical carcinoma and hepatoblastoma [7]. However, neonatal RMS associated with BWS is extremely rare [2].

To our knowledge, only 9 cases of RMS associated with BWS, including our case, have been reported [2,7,8-11]. The RMS subtype was alveolar in 5 patients, embryonal in 3, and unknown in 1. Of the 5 patients with alveolar RMS, 3 had multiple skin lesions (Table 1). In the genetic analyses of the cases of alveolar RMS, neither *PAX3-FKHR* nor *PAX7-FKHR* transcripts were reported to be present; however, hypomethylation of DMR-LIT1, indicating biallelic expression of *KCNQ1OT1*, was observed. Alveolar RMS has a poor prognosis because there was only 1 disease-free survivor.

On the other hand, 19 cases of neonatal alveolar RMS without BWS have been reported [12-19]. The patients were predominantly female infants, and the most common sites were the extremities. There were 11 cases (59%) of skin lesions, and brain metastasis was observed in 5 (45%) of these 11 patients. In the molecular analysis of samples from 7 patients, the *PAX3-FKHR* transcripts were observed in only 3 cases (43%) (Table 2). These data suggest that neonatal alveolar RMS has a tendency to develop as multiple skin lesions associated with brain metastasis and that common translocations are not observed frequently in this condition. The overall survival rate was 26%, and only 3 patients (15.8%) were disease-free. In particular, neonates with skin lesions had a poorer prognosis than those without lesions. Therefore, we should consider the possibility of malignant neoplastic disease when diagnosing the neonatal skin lesions that present as a plaque-like or nodular lesion with slow but progressive growth [13-15].

This report is the first to demonstrate an association between BWS and primary cutaneous alveolar RMS in a neonate. Furthermore, this case is of interest not only for the unique clinical presentation but also for the absence of the

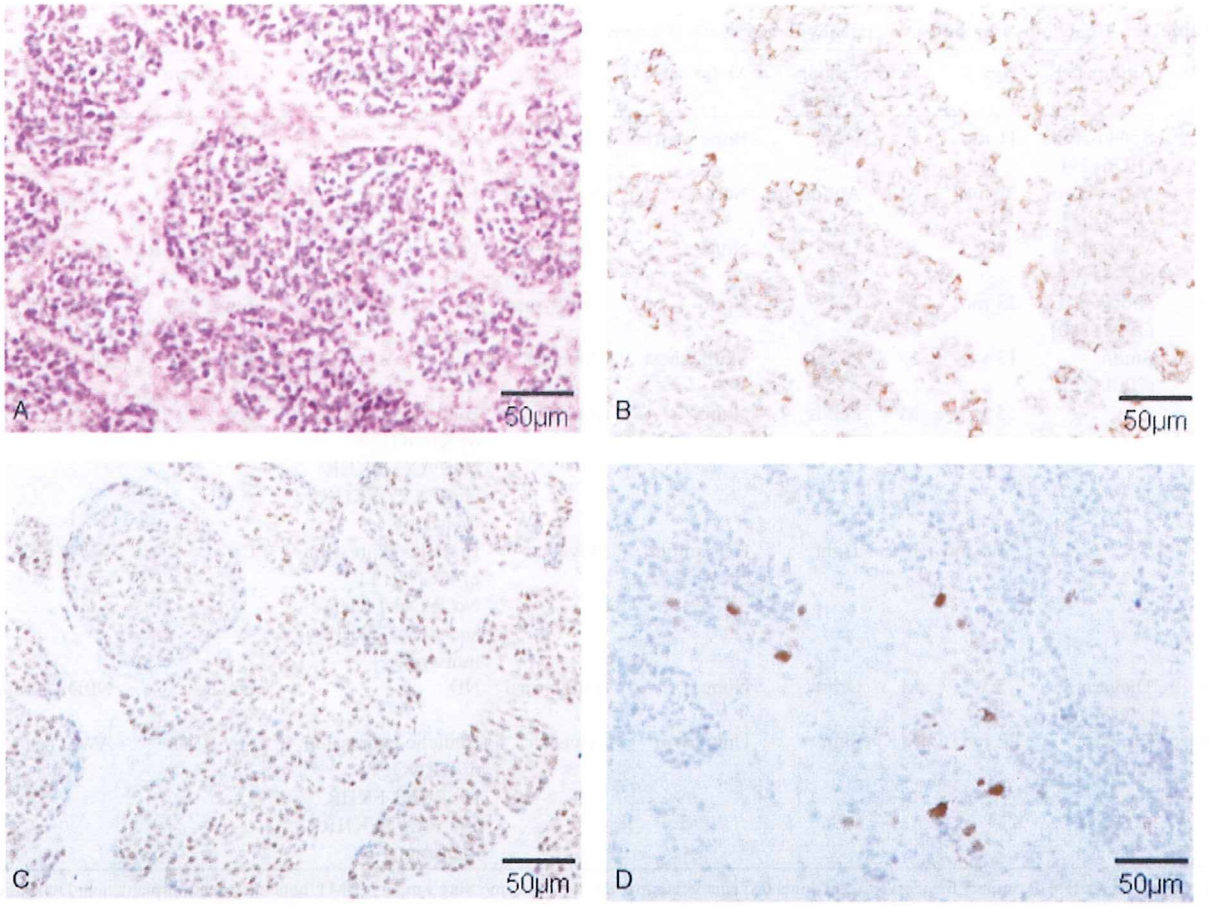

Fig. 2 Pathological features of the tumor. The tumor cells were undifferentiated with very little cytoplasm (A, hematoxylin and eosin; original magnification ×200). Immunohistochemical studies revealed that the tumor cells were positive for desmin (B, original magnification ×200), myogenin (C, original magnification ×200), and myoglobin (in the focal areas; D, original magnification ×200).

fusion transcripts. The absence of these common translocations in spite of the presence of the DMR-LIT1 demethylation, which is indicative of biallelic expression of *KCNQ1OT1*, indicates that the antisense transcript on 11p15 may be involved in an alternate pathway that leads to the development of alveolar RMS.

Acknowledgment

We thank Professor Hidenobu Soejima and Dr Kensaku Sasaki (Division of Molecular Biology and Genetics, Department of Biomolecular Sciences, Faculty of Medicine, Saga University, Japan) for conducting the molecular analyses.

References

[1] Wiedemann HR. Familial malformation complex with umbilical hernia and macroglossia—a "new syndrome"? J Genet Hum 1964;13:223-32.

[2] Smith AC, Squire JA, Thorner P, et al. Association of alveolar rhabdomyosarcoma with the Beckwith-Wiedemann syndrome. Pediatr Dev Pathol 2001;4:550-8.

[3] Maher ER, Reik W. Beckwith-Wiedemann syndrome: imprinting in clusters revisited. J Clin Invest 2000;105:247-52.

[4] Lee MP, DeBaun MR, Mitsuya K, et al. Loss of imprinting of a paternally expressed transcript, with antisense orientation to KVLQT1, occurs frequently in Beckwith-Wiedemann syndrome and is independent of insulin growth factor II imprinting. Proc Natl Acad Sci USA 1999;96:5203-8.

[5] Engel JR, Smallwood A, Harper A, et al. Epigenotype-phenotype correlations in Beckwith-Wiedemann syndrome. J Med Genet 2000; 37:921-6.

[6] Wiedemann HR. Tumors and hemihypertrophy associated with the Wiedemann-Beckwith syndrome. Eur J Pediatr 1983;141:129.

[7] Sotelo-Avila C, Gooch III WM. Neoplasms associated with the Beckwith-Wiedemann syndrome. Perspect Pediatr Pathol 1976;3: 255-72.

[8] Matsumoto T, Kinoshita E, Maeda H, et al. Molecular analysis of a patient with Beckwith-Wiedemann syndrome, rhabdomyosarcoma and renal cell carcinoma. Jpn J Human Genet 1994;39: 225-34.

[9] Vaughan WG, Sanders DW, Grosfeld JL, et al. Favorable outcome in children with Beckwith-Wiedemann syndrome and intraabdominal malignant tumors. J Pediatr Surg 1995;30: 1042-5.

[10] Aideyan UO, Kao SC. Case report: Urinary bladder rhabdomyosarcoma associated with Beckwith-Wiedemann syndrome. Clin Radiol 1998;53:457-9.

Table 1 Rhabdomyosarcoma associated with Beckwith-Wiedemann syndrome

No.	Author (y)	Age	Sex	Primary Tumor	Metastasis	Histology	Molecular Pathology	Treatment	Outcome
1	Sotelo-Avila (1976) [7]	11 mo	F	Orbit	Bone marrow	Alveolar	ND	Cx, Rx	DOD (16 mo)
2	Matsumoto (1994) [8]	22 mo	M	Abdomen	None	Embryonal	ND	Cx, Surg	Unknown
3	Vaughan (1995) [9]	3 y	F	UB	None	Unknown	ND	Surg, Cx, Rx	Alive (20 mo)
4	Aideyan (1998) [10]	23 mo	M	UB	None	Embryonal	ND	Surg, Cx	DOD (25 mo)
5	Smith (2001) [2]	13 y	F	Cheek	Skull, chest	Alveolar	ND	Rx	DOD (8 mo)
6		5 y	M	Pelvis	None	Alveolar	Biallelic expression of KCNQ1T1 No PAX3-FKHR and PAX7-FKHR transcript	Cx	NED (16 y)
7		1.5 mo	F	Tight	Extremities, chest	Alveolar	Biallelic expression of KCNQ1T1 No PAX3-FKHR and PAX7-FKHR transcript	Cx	AWD (?)
8	Thavaraj (2002) [11]	5 y	M	Orbit	None	Embryonal	ND	Cx, Rx	NED (20 mo)
9	Our case (2005)	22 d	M	Skin	Unknown	Alveolar	Biallelic expression of KCNQ1T1 No PAX3-FKHR and PAX7-FKHR transcript	Cx, BMT	AWD (?)

F, female; M, male; UB, urinary bladder; ND, not done; Cx, chemotherapy; Rx, radiotherapy; Surg, surgery; BMT, bone marrow transplantation; DOD, died of disease; AWD, alive with disease; NED, no evidence of disease.

[11] Thavaraj V, Sethi A, Arya LS. Incomplete Beckwith-Wiedemann syndrome in a child with orbital rhabdomyosarcoma. Indian Pediatr 2002;39:299-304.

[12] Grundy R, Anderson J, Gaze M, et al. Congenital alveolar rhabdomyosarcoma: Clinical and molecular distinction from alveolar rhabdomyosarcoma in older children. Cancer 2001;91:606-12.

[13] Kitagawa N, Arata J, Ohtsuki Y, et al. Congenital alveolar rhabdomyosarcoma presenting as a Blueberry Muffin Baby. J Dermatol 1989;16:409-11.

[14] Godambe SV, Rawal J. Blueberry muffin rash as a presentation of alveolar cell rhabdomyosarcoma in a neonate. Acta Pædiatr 2000;89: 115-7.

[15] Rodriguez-Galindo C, Hill DA, Onyekwere O, et al. Neonatal alveolar rhabdomyosarcoma with skin and brain metastases. Cancer 2001;92: 1613-20.

[16] Brecher AR, Reyes-Mugica M, Kamino H, et al. Congenital primary cutaneous rhabdomyosarcoma in a neonate. Pediatr Dermatol 2003;20: 335-8.

[17] Romos-Perea C, Fernandez-Sein A, Bonet N, et al. Congenital orbital alveolara rhabdomyosarcoma. Bol Asoc Med PR 1983;75:481-3.

[18] Campbell AN, Chan HSL, O'Brien A, et al. Malingnant tumors in the neonate. Arch Dis Child 1987;62:19-23.

[19] Schmidt D, Fletcher CDM, Harms D. Rhabdomyosarcomas with primary presentation in the skin. Path Res Pract 1993;189:422-7.